DOI: 10.1002/chem.200601856

Structure, Stability, Dynamics, High-Field Relaxivity and Ternary-Complex Formation of a New Tris(aquo) Gadolinium Complex

Aline Nonat, Pascal H. Fries, Jacques Pécaut, and Marinella Mazzanti*[a]

Abstract: The tripodal hexadentate picolinate ligand dpaa^{3-} (H_3dpaa = *N*,*N*′-bis[(6-carboxypyridin-2-yl)methyl]glycine) has been synthesised. It can form 1:1 and 1:2 lanthanide/ligand complexes. The crystal structure of the bis(aquo) lutetium complex [Lu(dpaa)$(H_2O)_2$] has been determined by X-ray diffraction studies. The number of water molecules was determined by luminescence lifetime studies of the terbium and europium complexes. The tris(aquo) terbium complex shows a fairly high luminescence quantum yield (22%). The [Gd(dpaa)$(H_2O)_3$] complex displays a high water solubility and an increased stability (pGd = 12.3) with respect to the analogous bis(aquo) complex [Gd(tpaa)$(H_2O)_2$] (pGd = 11.2). Potentiometric and relaxometric studies show the formation of a soluble Gd^{III} hydroxo complex at high pH values. A unique aquohydroxo gadolinium complex has been isolated and its crystal structure determined. This complex crystallises as a 1D polymeric chain consisting of square-shaped tetrameric units. In heavy water, the [Gd(dpaa)$(D_2O)_3$] complex shows a quite high HOD proton relaxivity at high field (11.93 s^{-1} mM^{-1} at 200 MHz and 298 K) because of the three inner-sphere water molecules. The formation of ternary complexes with physiological anions has been monitored by relaxometric studies, which indicate that even under conditions favourable to the formation of adducts with oxyanions, the mean relaxivity remains higher than those of most of the currently used commercial contrast agents except for the citrate. However, the measured relaxivity ($\bar{r}_1 = 7.9$ s^{-1} mM^{-1}) in a solution containing equimolar concentrations of [Gd(dpaa)$(D_2O)_3$] and citrate is still high. The interaction with albumin has been investigated by relaxometric and luminescence studies. Finally, a new versatile method to unravel the geometric and dynamic molecular factors that explain the high-field relaxivities has been developed. This approach uses a small, uncharged non-coordinating probe solute, the outer-sphere relaxivity of which mimics that of the water proton. Only a routine NMR spectrometer and simple mathematical analysis are required.

Keywords: chelates · gadolinium · imaging agents · lanthanides · N ligands

Introduction

Magnetic resonance imaging (MRI) has become one of the most important diagnostic techniques in medicine, and MRI application in molecular imaging is foreseen. Gadolinium complexes are frequently used to improve contrast in medical examinations as a result of their ability to increase the relaxation rates of water protons in tissue.[1] All the gadolinium complexes currently used as contrast agents have only one water molecule coordinated to the metal and show low relaxivity ($r_1 = 4.5$ s^{-1} mM^{-1}; 20 MHz, 298 K) relative to the theoretically attainable maximum. The application of MRI to the detection of a specific molecular target requires the design of contrast agents with much higher relaxivity.[2–4] For that purpose, all the molecular parameters that determine the relaxivity (the number q of water molecules bound to the gadolinium centre, the longitudinal relaxation time T_{1e} of the metal electronic spin, the rotational correlation time τ_R of the complex and the exchange rate k_{ex} of a coordinated water molecule) should be simultaneously optimised at the desired field.

Of particular current interest is the development of contrast agents that display high relaxivity at the field values of the new imaging instruments (3T–5T). A higher relaxivity can be achieved by increasing the number of water mole-

[a] Dr. A. Nonat, Dr. P. H. Fries, Dr. J. Pécaut, Dr. M. Mazzanti
Laboratoire de Reconnaissance Ionique and Chimie de Coordination
Service de Chimie Inorganique et Biologique (UMR-E 3 CEA-UJF)
Département de Recherche Fondamentale sur la Matière Condensée
SCIB/DRFMC/DSM CEA-Grenoble, 17 rue des Martyrs
38054 Grenoble, Cedex 09 (France)
Fax: (+33) 438-785-090
E-mail: marinella.mazzanti@cea.fr

Supporting information for this article is available on the WWW under http://www.chemeurj.org/ or from the author.

cules in the first coordination sphere and the second-sphere contribution,[5,6] as these factors are favourable at all field values. Despite the large relaxivity enhancement associated with the increase of the number q of gadolinium-bound water molecules, only limited efforts have been directed to the development of gadolinium complexes with more than one metal-bound water molecule.[7] This is due to the expected decreased thermodynamic stability of these systems that could lead to toxicity in vivo. In addition, endogenous anions and/or side-chain carboxylate groups of the proteins, such as serum albumin, may cause a partial or total displacement of the coordinated water molecules of the bis- and tris-(aquo) complexes, thus suppressing the relaxivity enhancement benefit as a result of the high number of these water molecules in the free complex.[8–13] For example, the interaction of the gadolinium complexes of the macrocyclic heptadentate ligand do3a^{3-} (H_3do3a = 1,4,7,10-tetraazacyclododecane-1,4,7-triacetic acid) and its derivatives with carbonate, phosphate, citrate, malonate or lactate groups leads to the displacement of at least one inner-sphere water molecule.[14,15] Strong phosphate binding dramatically decreases the relaxivity of gadolinium complexes of hexadentate texaphyrins from 17 to 5 s^{-1} mM^{-1}.[16]

Over the last few years, however, a small number of very promising $q = 2$ gadolinium complexes have been reported.[17–19] The introduction of three additional carboxylate groups on the heptadentate do3a^{3-} ligand suppresses anionic binding to the gadolinium centre by electrostatic repulsion.[17] Recent studies of complexes of the tripodal hydroxypyridone (HOPO)-based ligands show that a high number of inner-sphere water molecules does not necessarily imply their ready displacement by physiological anions, even in neutral or cationic complexes.[20,21] This behaviour indicates that an appropriate choice of the coordination geometry can prevent physiological anion binding in complexes with more than one inner-sphere water molecule and suggests that the tripodal geometry might be particularly suitable for the design of gadolinium-based contrast agents with several inner-sphere water molecules.

Gadolinium complexes of polydentate ligands containing picolinate chelating groups have shown interesting relaxation properties.[22–28] In particular, the gadolinium complex of the heptadentate tripodal ligand tpaa (H_3tpaa = α,α′,α″-nitrilotri(6-methyl-2-pyridinecarboxylic acid); Scheme 1) containing three picolinate arms connected to a nitrogen atom[29,30] has a relaxivity more than twofold higher than the relaxivities of the clinically used current contrast agents based on monoaqua complexes of octa-coordinate ligands.

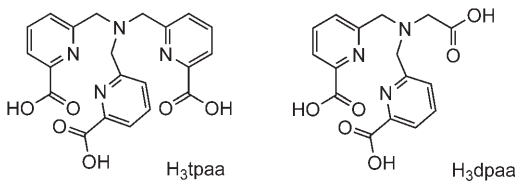

Scheme 1. Ligands H_3tpaa and H_3dpaa.

However, the in-depth investigation of the properties of this complex and its application as a contrast agent are impossible as a result of its low water solubility. Herein, we describe the synthesis, structure, stability and relaxivity of the new tris(aquo) gadolinium complex of the tripodal hexadentate picolinate ligand dpaa^{3-} (H_3dpaa = *N*,*N*′-bis[(6-carboxypyridin-2-yl)methyl]glycine; Scheme 1). The picolinate [Gd(dpaa)$(H_2O)_3$] complex displays a high water solubility and an increased stability with respect to the [Gd(tpaa)$(H_2O)_2$] complex in spite of the lower denticity of dpaa^{3-} relative to tpaa^{3-}. The relaxivity of the 1:2 lanthanide/ligand complex [Gd(dpaa)$_2(H_2O)]^{3-}$ is also described. The relaxivity change induced by most of the physiological anions and bovine serum albumin is investigated by relaxometric and luminescence studies. At a high pH value, a unique aquohydroxo gadolinium complex has been isolated and its crystal structure determined. A new practical method to analyse the geometric and dynamic molecular factors that explain the relaxivities measured at high field is also presented in detail.

Results and Discussion

Synthesis: *N*,*N*′-Bis[(6-carboxypyridin-2-yl)methyl]glycine (H_3dpaa) was obtained in two steps with a global yield of 38% from the previously described 6-chloromethylpyridine-2-carboxylic acid ethyl ester. The ^{1}H NMR spectrum of H_3dpaa in D_2O at pD = 4.7 displays a single set of five signals that imply C_{2v} symmetry. The [Gd(dpaa)$(H_2O)_3$] and [Lu(dpaa)$(H_2O)_2$] complexes were prepared by reaction of the corresponding lanthanide chloride and H_3dpaa ligands in water at pH ≈ 5–6 (adjusted with KOH). Satisfactory elemental analyses were obtained after elimination of the salts.

Crystal structure of the dpaa complexes: X-ray-quality crystals of the lutetium complex were obtained by slow evaporation of 1:1 solutions of $LnCl_3$ and H_3dpaa in water after adjustment of the pH value to 5.27. The ORTEP diagram of [Lu(dpaa)$(H_2O)_2$] (**2**) is shown in Figure 1 and its crystallographic data are presented in Tables 1 and 2. The Lu ion is octa-coordinate by the hexadentate ligand dpaa and two water molecules. The geometry can be described as a slightly distorted dodecahedron. The crystal structures of the Ln^{III} complexes of the analogous tpaa^{3-} ligand[30] vary along the series with respect to their nuclearity and the number of water molecules coordinated to the metal centre, with a tetrameric structure observed for the La^{3+} ion (nine- and ten-coordinate metal centres), dimeric structures formed from the Nd^{3+} ion through the Yb^{3+} ion (nine-coordinate complexes) and a monomeric structure for the Lu^{3+} ion (eight-coordinate with one bound water molecule). The value of Lu–N_{apical} (2.575(11) Å) in **2** is very similar to the value found for Lu–N_{apical} (2.6071(18) Å) in the eight-coordinate complex [Lu(tpaa)$(H_2O)]\cdot 4H_2O$ and for Lu–N_{apical} (2.555(1) Å) in the hepta-coordinate complex [Lu(tpa)Cl_3] (tpa = tris[(2-pyridyl)methyl]amine).[31] The three arms of the dpaa ligand adopt a pincer-like arrangement around the

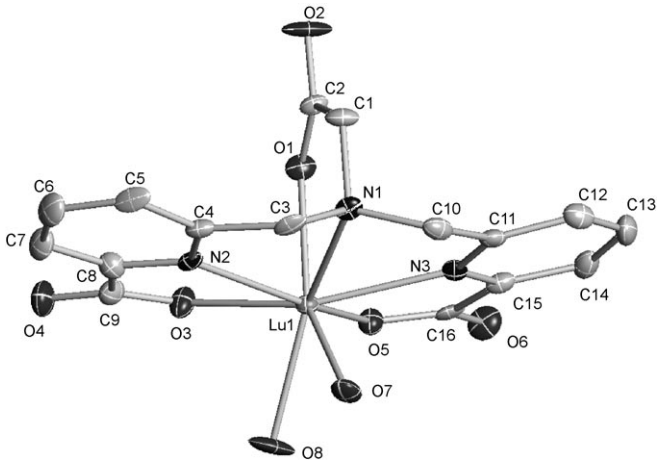

Figure 1. ORTEP diagram of the complex $[Lu(dpaa)(H_2O)_2]$ (**2**), with thermal ellipsoids at 30% probability.

Table 1. Crystallographic data for the structures.

	2	**3**
formula	$C_{16}H_{20}LuN_3O_{10}$	$C_{65}H_{89}Gd_4N_{12}Na_3O_{45}$
M_r	589.32	2456.46
crystal system	monoclinic	monoclinic
space group	$P2(1)/n$	$P\bar{1}$
a [Å]	8.042(4)	12.440(2)
b [Å]	11.948(7)	13.625(2)
c [Å]	14.985(6)	14.310(2)
α [Å]	90	83.439(2)
β [Å]	100.40(1)	66.688(2)
γ [Å]	90	80.559(2)
V [Å^3/Z]	1878(3)/4	2194.1(5)/2
λ	0.71073	0.71073
ρ_{calcd} [g cm^{-3}]	1.712	1.859
$\mu(Mo_{K\alpha})$ [mm^{-1}]	1.898	3.101
t [K]	223(2)	223(2)
R_1, wR_2[a]	0.0414, 0.0854	0.0320, 0.0751

[a] Structure was refined on F_0^2 using all data : $wR_2=[\Sigma[w(F_0^2-F_c^2)^2]/\Sigma w(F_0^2)^2]^{1/2}$, where $w^{-1}=[\Sigma(F_0^2)+(aP)^2+bP]$ and $P=[\max(F_0^2, 0)+2F_c^2]/3$.

Table 2. Selected bond lengths [Å] and angles [°] in **2**.

Lu1–O1	2.251(10)	Lu1–O5	2.262(9)	Lu1–O3	2.289(9)
Lu1–O7	2.327(10)	Lu1–O8	2.337(9)	Lu1–N2	2.397(10)
Lu1–N3	2.399(10)	Lu1–N1	2.575(11)		
O1-Lu1-O5	83.2(3)	O1-Lu1-O3	78.7(3)	O5-Lu1-O3	86.3(3)
O1-Lu1-O7	142.5(3)	O5-Lu1-O7	119.2(3)	O3-Lu1-O7	128.7(3)
O1-Lu1-O8	149.2(3)	O5-Lu1-O8	81.1(4)	O3-Lu1-O8	74.0(4)
O7-Lu1-O8	68.1(4)	O1-Lu1-N2	81.7(3)	O5-Lu1-N2	152.1(3)
O3-Lu1-N2	67.9(3)	O7-Lu1-N2	86.4(3)	O8-Lu1-N2	100.5(4)
O1-Lu1-N3	80.9(3)	O5-Lu1-N3	68.4(3)	O3-Lu1-N3	149.0(4)
O7-Lu1-N3	80.7(3)	O8-Lu1-N3	117.0(4)	N2-Lu1-N3	131.3(4)
O1-Lu1-N1	70.9(3)	O5-Lu1-N1	129.7(3)	O3-Lu1-N1	127.2(3)
O7-Lu1-N1	71.8(3)	O8-Lu1-N1	138.3(3)	N2-Lu1-N1	65.9(3)
N3-Lu1-N1	65.5(3)				

metal centre, whereas the three picolinate arms adopt a helical arrangement in the $tpaa^{3-}$ complex. This behaviour does not lead to significant differences in the Lu–$O_{carboxy}$ bond length (mean values: 2.27(2) and 2.30(4) Å in Lu(dpaa) and Lu(tpaa), respectively) and the Lu–N bond length (mean values: 2.46(1) and 2.48(9) Å in Lu(dpaa) and Lu(tpaa), respectively).

Obtaining crystals of the gadolinium complex at low pH values was prevented by its high water solubility. X-ray-quality crystals of the gadolinium complex were only obtained by slow evaporation of a 1:1 solution of $[Gd(OTf)_3]$ (OTf = triflate) and $dpaa^{3-}$ at pH ≈ 8. X-ray diffraction studies revealed the presence of two sets of two independent gadolinium complexes connected by bridging carboxylate units to form a centrosymmetric tetramer with a square-shaped arrangement (Figure 2). Both gadolinium complexes are

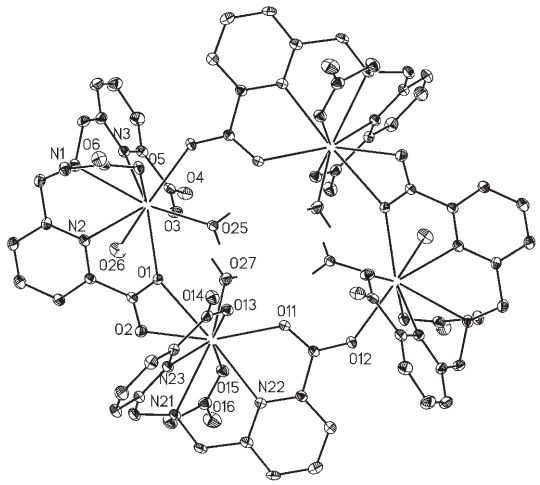

Figure 2. ORTEP diagram of the anion $[\{Gd(dpaa)(H_2O)_2\}_2\{Gd(dpaa)(H_2O)(OH)\}_2]^{2-}$ in **3**, with thermal ellipsoids at 30% probability.

nine-coordinate with a capped square-antiprism geometry, except for Gd1 the polyhedron is very distorted. The Gd2 centre is coordinated by the six donor atoms of the $dpaa^{3-}$ ligand, a water molecule and two oxygen atoms of the picolinate group from one of the adjacent gadolinium complexes. The carboxylate group bridges the two gadolinium ions in a $\mu:\eta^1;\eta^2$ fashion. This behaviour suggests that the geometry of the coordinated ligand does not prevent the binding of additional carboxylate groups in a η^2 fashion. The picolinate oxygen atom not involved in the coordination of Gd2 binds the other adjacent Gd1 complex in a $\mu:\eta^1;\eta^1$ fashion. The gadolinium ion Gd1 is coordinated by the six donor atoms of the $dpaa^{3-}$ ligand, a picolinate oxygen atom from the adjacent gadolinium complex, one oxygen atom for a water molecule and one oxygen atom from a hydroxide species. The bridging hydroxide moiety is also coordinated to a sodium cation. A six-coordinate sodium centre binds the carboxylate oxygen atoms of two acetate arms from the gadolinium complexes of different tetrameric units, thus leading to the formation of the infinite 1D polymer $[\{[Gd(dpaa)(H_2O)]_2\{[Gd(dpaa)(H_2O)(OH)]Na(H_2O)_2\}_2\}2\text{-}Na(OH)(H_2O)_3\cdot CH_3OH\cdot 6H_2O]_\infty$ (**3**, see Figure 3 for the ORTEP diagram and Tables 1 and 3 for its crystallographic data).

The four remaining coordination sites of the sodium cation are occupied by two water molecules and a hydroxide

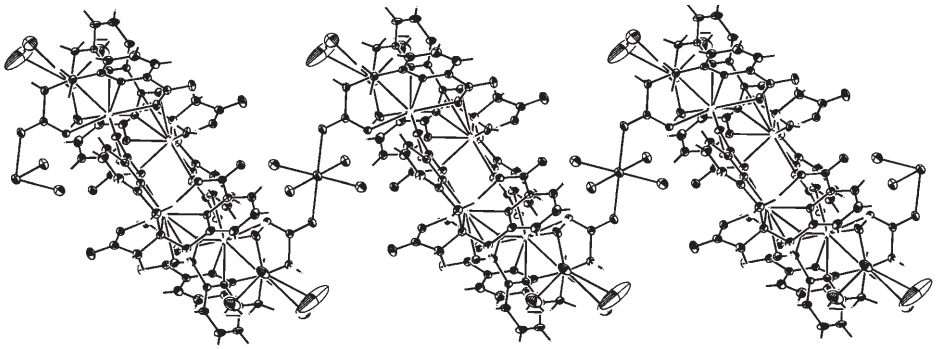

Figure 3. ORTEP diagram of the 1D polymeric structure of **3**, with thermal ellipsoids at 30% probability.

Table 3. Selected bond lengths [Å] and angles [°] in **3**.[a]

Gd1−O25	2.382(3)	Gd1−O5	2.403(3)	Gd1−O3	2.412(3)
Gd1−O12#1	2.418(3)	Gd1−O26	2.422(3)	Gd1−O1	2.478(3)
Gd1−N2	2.523(3)	Gd1−N3	2.571(3)	Gd1−N1	2.666(3)
Gd2−O15	2.340(3)	Gd2−O11	2.386(3)	Gd2−O27	2.396(3)
Gd2−O13	2.421(3)	Gd2−O2	2.467(3)	Gd2−N23	2.562(3)
Gd2−N22	2.581(3)	Gd2−O1	2.637(3)	Gd2−N21	2.695(3)
O25-Gd1-O5	85.67(11)	O25-Gd1-O3	88.18(11)	O5-Gd1-O3	151.34(10)
O25-Gd1-O12#1	73.44(11)	O5-Gd1-O12#1	71.74(10)	O3-Gd1-O12#1	79.67(10)
O25-Gd1-O26	85.83(12)	O5-Gd1-O26	69.86(11)	O3-Gd1-O26	137.54(11)
O12#1-Gd1-O26	137.37(11)	O25-Gd1-O1	72.25(10)	O5-Gd1-O1	134.99(9)
O3-Gd1-O1	68.30(9)	O12#1-Gd1-O1	133.10(9)	O26-Gd1-O1	69.85(11)
O25-Gd1-N2	136.77(11)	O5-Gd1-N2	119.43(10)	O3-Gd1-N2	83.36(10)
O12#1-Gd1-N2	144.76(10)	O26-Gd1-N2	72.99(11)	O1-Gd1-N2	65.21(10)
O25-Gd1-N3	133.47(11)	O5-Gd1-N3	102.69(10)	O3-Gd1-N3	62.74(10)
O12#1-Gd1-N3	66.49(10)	O26-Gd1-N3	140.27(11)	O1-Gd1-N3	121.10(9)
N2-Gd1-N3	78.29(10)	O25-Gd1-N1	149.15(11)	O5-Gd1-N1	63.55(10)
O3-Gd1-N1	119.63(10)	O12#1-Gd1-N1	97.20(10)	O26-Gd1-N1	81.80(11)
O1-Gd1-N1	128.03(9)	N2-Gd1-N1	65.22(10)	N3-Gd1-N1	61.24(10)
O15-Gd2-O11	86.80(10)	O15-Gd2-O27	80.20(11)	O11-Gd2-O27	70.31(11)
O15-Gd2-O13	159.46(10)	O11-Gd2-O13	73.26(10)	O27-Gd2-O13	97.17(11)
O15-Gd2-O2	81.11(10)	O11-Gd2-O2	151.86(10)	O27-Gd2-O2	82.59(11)
O13-Gd2-O2	118.96(9)	O15-Gd2-N23	128.50(10)	O11-Gd2-N23	126.70(11)
O27-Gd2-N23	142.68(11)	O13-Gd2-N23	64.16(10)	O2-Gd2-N23	79.88(10)
O15-Gd2-N22	70.77(10)	O11-Gd2-N22	63.58(10)	O27-Gd2-N22	125.89(11)
O13-Gd2-N22	95.32(10)	O2-Gd2-N22	133.48(10)	N23-Gd2-N22	89.36(10)
O15-Gd2-O1	122.97(9)	O11-Gd2-O1	119.81(9)	O27-Gd2-O1	66.33(10)
O13-Gd2-O1	73.01(9)	O2-Gd2-O1	51.03(9)	N23-Gd2-O1	77.05(10)
N22-Gd2-O1	164.91(10)	O15-Gd2-N21	66.91(10)	O11-Gd2-N21	127.18(10)
O27-Gd2-N21	139.84(11)	O13-Gd2-N21	121.67(10)	O2-Gd2-N21	70.50(10)
N23-Gd2-N21	61.66(11)	N22-Gd2-N21	4.67(10)	O1-Gd2-N21	112.89(9)

[a] Symmetry transformations used to generate equivalent atoms: #1 $-x+1$, $-y+1$, $-z$.

ion. The presence of this hydroxide anion is necessary to balance the complex charge, although the position of the hydroxide species bound to the sodium ion cannot be assigned because the hydrogen atoms of the water molecules and the hydroxide were not localised probably as a result of disorder.

The presence of both the aquo and monohydroxo complexes in a ratio of 1:1 in the structure can be explained by the low solubility of this species and the potentiometric results, which indicate the presence of hydroxo species in solution with water above pH 8 (see below). The formation of soluble lanthanide–hydroxo complexes in the presence of neutral polyaminocarboxylate ligands has been observed in solution at high pH values.[32] Furthermore, the self-assembly of dinuclear, tetranuclear and dodecanuclear polymetallic hydroxo complexes has been reported for lanthanide–ethylenediaminetetraacetic acid (H_4edta) complexes under conditions of high pH (pH 13–14).[33] Mononuclear aquo–hydroxo complexes were suggested as probable intermediates in the mechanism proposed for the self-assembly of tetranuclear polyhydroxo complexes from their corresponding mononuclear aquo–hydroxo complex; however, these intermediates were never isolated. Moreover although several lanthanide–hydroxo complexes have been structurally characterised,[33–38] this example is a rare as the hydroxo ligand is not bridging two lanthanide centres.[39]

The described structure suggests that the $dpaa^{3-}$ ligand is a very good candidate for use in the ligand-controlled synthesis of polynuclear lanthanide–oxo/hydroxo complexes, and the lanthanide coordination chemistry of this ligand at high pH values could provide new structural motifs.

Protonation and stability constants: The protonation constants of H_3dpaa, defined as $K_{ai}=[H_iL]^{(3-i)-}/[H_{i-1}L]^{(4-i)-}[H^+]$, were determined to be $pK_{a3}=2.9(1)$, $pK_{a2}=3.8(1)$ and $pK_{a1}=7.33(3)$ (0.1 M KCl, 298 K) by potentiometric titration (the titration curves of H_3dpaa and its Gd^{III} complexes are presented in the Supporting Information). The highest pK_a value (7.33(3)) may be identified with the protonation of the nitrogen atom of the tertiary amine, followed by the protonation of the carboxylate groups of the picolinate moieties. The protonation of the remaining carboxylate group occurs at a lower pH value, and the associated pK_a value could not be determined. The values of pK_{a2} and pK_{a3} are consistent with the values found for the protonation of the picolinate carboxylate moiety in the tripodal ligand α,α′,α″-nitrilotri(6-methyl-2-pyridinecarboxylic acid (H_3tpaa; $pK_{a3}=3.3(1)$, $pK_{a2}=4.11(6)$).[30] The low value of $pK_{a1}=7.33$ relative to the value reported for nitrilotriethanoic acid (H_3nta;

$pK_{a1}=9.75$)[40] is due to the presence of two 6-methyl-2-pyridinecarboxylic acid groups and is consistent with the value of $pK_a=7.30$ reported for the nitrogen atom of the secondary amine in bis(2-pyridylmethyl)amine (dpa).[41]

The stability constants of the complexes formed between the Ln^{III} centre (Ln = Gd and Tb) and H_3dpaa were determined by direct titration of 1:1 Gd/H_3dpaa (4.3×10^{-4} M), 1:2 Gd/H_3dpaa (4.4×10^{-4} M), 1:1 Tb/H_3dpaa (3.6×10^{-4} M) and 1:2 Tb/H_3dpaa (1.8×10^{-4} M) mixtures in the pH range 2.5–10.3. The titration data could be fitted to the following equations [Eqs (1)–(3)]:

$$Gd^{3+} + dpaa^{3-} = [Gd(dpaa)] \quad \log K_{GdL} = 10.6(2) \tag{1}$$

$$[Gd(dpaa)] + dpaa^{3-} = [Gd(dpaa)_2)^{3-} \quad \log K_{GdL_2} = 6.0(3) \tag{2}$$

$$[Gd(dpaa)] + dpaaH^{2-} = [Gd(dpaa)(dpaaH)]^{2-} \quad \log K_{GdLLH} = 5.2(4) \tag{3}$$

$$Tb^{3+} + dpaa^{3-} = [Tb(dpaa)] \quad \log K_{TbL} = 10.4(2) \tag{1a}$$

$$[Tb(dpaa)] + dpaa^{3-} = [Tb(dpaa_2]^{3-} \quad \log K_{TbL_2} = 4.8(5) \tag{2a}$$

$$[Tb(dpaa)] + dpaaH^{2-} = [Tb(dpaa)(dpaaH)]^{2-} \quad \log K_{TbLLH} = 6.4(4) \tag{3a}$$

The value of pGd = 12.3 ($-\log[M]_{free}$ at pH 7.4, $[M]_{total}$ = 1 μM and $[dpaa]_{total}$ = 10 μM), which allows a straightforward comparison of the complex stabilities under physiological conditions, is significantly higher than the value found for the $tpaa^{3-}$ complex (pGd = 11.2). The increase in stability is consistent with the overall increase of the ligand pK_a values (ΣpK_a = 14.03 and 9.91 for $dpaa^{2-}$ and $tpaa^{3-}$, respectively). The titration curves show an inflection point above pH 8, which is due to the formation of hydroxo species above this pH value, as confirmed by simulation of the curves.

The introduction of the additional species $[M(dpaa)OH]^-$ into the fit of the titration curves does not result in a significant modification of the values of the formation constants of the mono- and bis(ligand) complexes as their formation occurs before pH 8.

The small concentration of hydroxo complex present at the investigated pH region, associated with a probable slow kinetic process, prevents an accurate determination of the formation constant of the hydroxo species. To obtain a better qualitative description of the system, we have, however, included the speciation in a pH range in which the error of the formation constant of the hydroxo complexes has little influence on the amount of hydroxo species present in solution (up to pH 9). The species distribution curves (Figure 4) show that at a stoichiometric 1:1 ratio of Gd/

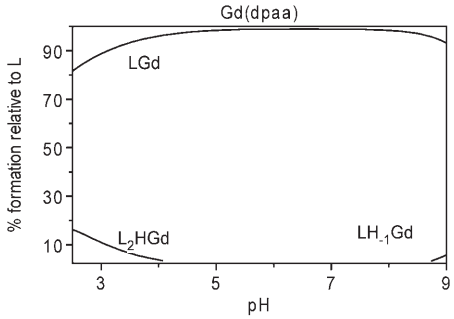

Figure 4. Gadolinium speciation in water (pH 2.5–9) in the presence of $dpaa^{3-}$ for $[Gd^{3+}]_{tot}=[dpaa]_{tot}$ = 0.44 mM. L = ligand.

$dpaa^{3-}$ dissociation of the complex occurs only below pH 4 and that at pH > 8 the soluble hydroxo species $[Gd(dpaa)(OH)]^-$ begins to form. At a stoichiometric 1:2 ratio of Gd/ligand, the distribution curve (Figure 5) shows that at above pH 7 and $[dpaa]_{total}$ = 0.22 mM the major solution species is the trianionic bis(ligand) complex $[Gd(dpaa)_2]^{3-}$ in which all the carboxylate oxygen atoms are deprotonated. Below pH 7, a dianionic monoprotonated form of the bis(ligand) complex is present. This complex is the major species at pH 4. At pH ≈ 7.5, the hydroxo species begins to form, thus displacing one $dpaa^{3-}$ ligand. Similar behaviour was observed for the terbium complex, and similar coordination behaviour was previously observed for ternary complexes of lanthanides with polyaminocarboxylate ligands.[42,43]

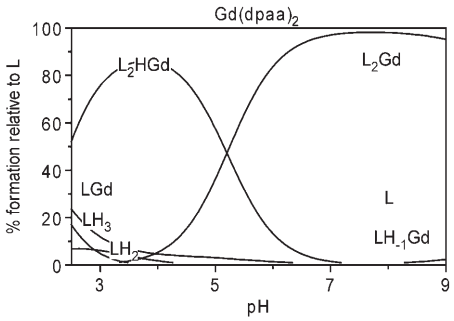

Figure 5. Speciation in water (pH 2.5–9) in the presence of $dpaa^{3-}$ for $[Gd^{3+}]_{tot}$ = 0.22 mM and $[dpaa]_{tot}$ = 0.44 mM.

Solution structure of the Ln^{III} complexes: The lanthanide complexes of $dpaa^{2-}$ show a very high solubility in water, which is different from the complexes of the heptadentate $tpaa^{3-}$ ligand as they are rather insoluble in water. As in both cases the complexes have neutral charges, the higher solubility probably arises from the removal of one pyridyl ring.

The ^{1}H NMR spectra (400 MHz) of [Ln(dpaa)] (Ln = La, Eu, Tb, Lu) complexes in D_2O at pD 6–8 and 298 K show the presence of only one set of signals for the pyridine protons, two signals for the diastereotopic methylene protons close to the pyridine ring and one resonance for the protons of the acetate group. This pattern is consistent with a C_s

symmetry of the species in solution, in which the two picolinate pendant arms are equivalent. The diastereotopic character of the CH_2 protons close to the pyridine ring indicates a long-lived coordination of the nitrogen atom of the ternary amine and is in agreement with a rigid C_s structure in solution. In contrast, for the analogous heptadentate $tpaa^{3-}$ ligand, fluxional C_{3v} species were observed in solution, as a consequence of a rapid interconversion between two different helical conformations (Δ and Λ). The different behaviour observed for the two ligands points to a better metal–ligand complementarity for the $dpaa^{3-}$ complexes.

Solution-structure NMR studies (400 MHz) were carried out on the $[Ln(dpaa)_2]^{3-}$ (Ln = Eu, Tb, Lu) complexes in D_2O at pD 6–8 and 298 K. Broad spectra were obtained for Ln = Tb and Lu, which is in agreement with the presence of conformational equilibria in solution. A more rigid spectrum was observed for the europium complex with more than 17 signals at 298 K for $[Eu(dpaa)_2]^{3-}$ (see the Supporting Information). This pattern indicates the presence of C_1-symmetric species in solution. Signal overlap prevented the attribution of the signals.

The solvation state of the mono- and bis(dpaa) complexes of Eu^{III} and Tb^{III} were studied by comparison of their luminescence decays in H_2O and D_2O. As a result of the different quenching efficiencies of the O–H and O–D oscillators, the measurement of Ln^{3+} phosphorescence lifetimes τ in solutions of H_2O and D_2O allows an accurate estimation of the number of coordinated water molecules present in solution q by using the equation of Beeby et al. ($q = A_{Ln}(1/\tau_{H_2O} - 1/\tau_{D_2O} - \alpha_{Ln})$ with $A_{Tb} = 5$ ms, $A_{Eu} = 1.2$ ms, $\alpha_{Tb} = 0.06\ ms^{-1}$ and $\alpha_{Eu} = 0.25\ ms^{-1}$;[44] this equation is a corrected version of the empirical equation of Horrocks and Sudnick,[45,46] thus accounting for closely diffusing OH oscillators). The observed lifetimes of the $Eu(^5D_0)$ ($\tau_{H_2O} = 0.307(2)$ ms and $\tau_{D_2O} = 2.53(2)$ ms) and Tb ($^5D_4$) ($\tau_{H_2O} = 0.99(1)$ ms and $\tau_{D_2O} = 2.65(3)$ ms) levels for the [Tb(dpaa)] and [Eu(dpaa)] complexes are in agreement with the presence of 3.1 ± 0.2 and 2.9 ± 0.2 coordinated water molecules in the Eu and Tb 1:1 complexes, respectively. A similar number of coordinated water molecules can be expected for the gadolinium ion, which has an ionic radius between those of the Eu and Tb ions. These results indicate the presence of monomeric tris(aquo) species in solution with water. The lifetimes of the $Eu(^5D_0)$ ($\tau_{H_2O} = 1.11(4)$ ms and $\tau_{D_2O} = 2.43(2)$ ms) and Tb ($^5D_4$) ($\tau_{H_2O} = 1.18(4)$ ms and $\tau_{D_2O} = 1.73(7)$ ms) levels measured under conditions ([Eu] $\approx 4.10^{-4}$ M and [dpaa] $\approx 8{,}8.10^{-4}$ M for Eu; [Tb] $\approx 1.10^{-3}$ M and [dpaa] $\approx 4.3.10^{-3}$ M for Tb) in which only the bis(dpaa) complexes $[Ln(dpaa)_2]^{3-}$ are present in solution are in agreement with the presence of 1.06 ± 0.2 and 0.3 ± 0.2 coordinated water molecules in the Tb and Eu complexes, respectively (Table 4). The q values reported for the Eu^{3+} and Tb^{3+} complexes of octadentate and nonadentate polyaminocarboxylate ligands are usually very similar.[7] However, luminescence decay rates of the free ions Tb^{3+} and Eu^{3+} in mixtures of D_2O and H_2O yielded values of $q = 9$ and 9.6 for terbium and europium, respectively.[47] Moreover systematic crystallographic studies of lanthanide complexes show that the change of coordination number occurs at different atomic numbers depending on the coordinated ligand. For example, the change in the number of coordinated water molecules occurs at the Tm centre for $[Ln(dota)(H_2O)_x]$ (dota = 1,4,7,10-tetraazacyclododecane-*N*,*N*′,*N*″,*N*‴-tetraacetic acid) complexes,[48] but at the Gd centre for the series of $[Ln(terpyridine)(NO_3)_2(H_2O)_x]NO_3$ ($x = 3$ for La–Gd and $x = 2$ for Tb–Lu) complexes.[49]

Table 4. Lifetime and absolute quantum yields in Tris buffer (pH 7.4, 298 K) relative to $[Eu(dpa)_3]^{3-}$ and $[Tb(dpa)_3]^{3-}$.

Compound	λ_{exc} [nm]	ε [$M^{-1}\,cm^{-1}$]	τ_{H_2O} [ms]	τ_{H_2O} [ms]	Θ_{H_2O} [%]	Θ_{D_2O} [%]
dpaa	268	8968	–	–	–	–
[Eu(dpaa)]	272	8940	0.307(2)	2.53(2)	1.5(3)	13(2)
[Tb(dpaa)]	272	8503	0.99(1)	2.65(3)	22(4)	54(8)
$[Eu(dpaa)_2]$	271	–	1.11(4)	2.43(2)	–	–
$[Tb(dpaa)_2]$	271	–	1.18(4)	1.73(7)	–	–

The different number of water molecules observed for the bis(dpaa) complexes can be interpreted in terms of important structural differences for these complexes. A possible explanation for the presence of a coordinated water molecule in the terbium complex is that a smaller number of donor atoms of the dpaa ligand is bound to the smaller terbium ion, thus leaving a coordination site available to bind a water molecule. The higher fluxional behaviour of the terbium complex observed by NMR spectroscopic analysis is in agreement with this interpretation.

Important differences in the formation mechanisms of ternary adducts Ln-edta-nta (nta = nitrilotriacetato) have been previously reported along the lanthanide series.[42,50] The high value of relaxivity measured for $[Gd(dpaa)_2]^{3-}$ ($r_{1p} = 6.4\ mM^{-1}s^{-1}$ at 200 MHz, 298 K) is in agreement with the presence of a coordinated water molecule, as observed for the terbium complex.

Relaxometric properties: The efficiency of a Gd^{III} complex to enhance the contrast of T_1-weighted magnetic resonance images is gauged by its relaxivity r_1, which is defined as the paramagnetic relaxation enhancement of the longitudinal relaxation rate of the water protons as a result of a 1 mM increase in the concentration of this complex at a given temperature and magnetic field.[1,7,51] The determination and analysis of the relaxometric parameters at high field were performed with a new method, which is described in the Theory Section and provides a simple and straightforward way of characterising the relaxivity performances of new gadolinium complexes at high field.

Relaxivity analysis of the Gd^{III} complexes: The relaxation rates of the HOD and CH_3OD protons were measured at 200 MHz and 298 K in solutions of $[Gd(dpaa)(D_2O)_3]$ and $[Gd(dpaa)_2(D_2O)]^{3-}$ in D_2O (Tables 5 and 6). First, consider the solution of $[Gd(dpaa)(D_2O)_3]$ as a worked example, for which the practical method of using the high-field relaxivity theory presented in the Theory Section is detailed in five

Table 5. The mixed OS proton relaxivities r_{mix}^{OS} at 200 MHz of a dilute uncharged probe solute CH_3OD that result from solutions of the complexes $[Gd(dpaa)(D_2O)_3]$ and $[Gd(dpaa)_2(D_2O)]^{3-}$ in D_2O at 298 K.[a]

	$[Gd(dpaa)(D_2O)_3]$	$[Gd(dpaa)_2(D_2O)]^{3-}$
T_1 [ms]	72.60	85.60
T_2 [ms]	56.90	68.30
$T_{1,\sigma}$ [ms]	56.90	67.60
$r_{mix,2}^{OS}$ [s^{-1} mM^{-1}]	3.74	3.09
$r_{mix,1\rho}^{OS}$ [s^{-1} mM^{-1}]	3.74	3.14
r_{mix}^{OS} [s^{-1} mM^{-1}]	3.74	3.12

[a] The concentrations of the complexes $[Gd(dpaa)(D_2O)_3]$ and $[Gd(dpaa)_2(D_2O)]^{3-}$ are 4.26 and 4.25 mM, respectively. The experimental proton relaxation times in the absence of Gd^{III} complexes are $T_{10}=9.43$ s $\cong T_{20}\cong T_{1,\sigma 0}$. The values of $r_{mix,2}^{OS}$ (respectively $r_{mix,1\rho}^{OS}$) are obtained from the measured longitudinal and transverse (respectively longitudinal in the rotating frame) relaxation times T_1 and T_2 (respectively $T_{1,\sigma}$). The arithmetic mean of $r_{mix,2\rho}^{OS}$ and $r_{mix,1\rho}^{OS}$ is $r_{mix}^{OS}\equiv(r_{mix,2}^{OS}+r_{mix,1\rho}^{OS})/2$.

Table 6. Relaxivity properties of the HOD protons at 200 MHz that arise from solutions of the complexes $[Gd(dpaa)(D_2O)_3]$ and $[Gd(dpaa)_2(D_2O)]^{3-}$ in D_2O at 298 K (the rotational correlation time τ_R and coordination lifetime τ_M are also reported).[a]

	$[Gd(dpaa)(D_2O)_3]$	$[Gd(dpaa)_2(D_2O)]^{3-}$
T_1 [ms]	19.64	31.91
T_2 [ms]	16.42	27.24
r_1 [s^{-1} mM^{-1}]	11.93	7.36
r_2 [s^{-1} mM^{-1}]	14.28	8.62
r_{mix}^{OS} [s^{-1} mM^{-1}]	2.84	2.24
r_1^{IS} [s^{-1} mM^{-1}]	9.40	5.45
r_2^{IS} [s^{-1} mM^{-1}]	11.12	6.17
τ_R [ps]	103.00	206.00
τ_M [μs]	0.10	0.45

[a] The concentrations of the complexes $[Gd(dpaa)(D_2O)_3]$ and $[Gd(dpaa)_2(D_2O)]^{3-}$ are 4.26 and 4.25 mM, respectively. The experimental proton relaxation times in the absence of Gd^{III} complexes are $T_{10}=12.5$ s $\cong T_{20}$. The total longitudinal and transverse relaxivities r_1 and r_2 are obtained from the measured relaxation times T_1 and T_2. The mixed OS relaxivity $r_{mix}{}^{OS}$ is estimated from its counterpart of the CH_3OD protons reported in Table 5, as explained in the relaxivity analysis section. This value is used to derive the longitudinal and transverse OS relaxivities $r_1{}^{OS}$ and $r_2{}^{OS}$, from which the IS contributions $r_1{}^{IS}$ and $r_2{}^{IS}$ to the total relaxivities are obtained as differences.

steps. The explanations are self-contained to make the theory readily usable for the characterisation of contrast agents. The complex $[Gd(dpaa)(D_2O)_3]$ is simply denoted by Gd(dpaa) in the mathematical symbols to simplify the notation. The equations are written in terms of the longitudinal and transverse relaxation times T_1 and T_2, but the same procedure holds when replacing T_2 with $T_{1\rho}$. The analysis begins with the interpretation of the CH_3OD proton relaxivities, which are of purely outer-sphere (OS) origin, because the inner-sphere (IS) contributions should be negligible as methanol coordinates to the Gd^{III} centre weakly at most.

Step 1 consists of deriving the experimental mixed relaxivity of the methanol (m) CH_3OD protons from Equation (4) [which is the expanded form of Equation (23) from the theory section in terms of directly measured properties]:

$$r_{mix,m}^{OS}(\infty)=\frac{3}{2}\left[\left(\frac{1}{T_2}-\frac{1}{T_{20}}\right)-\frac{1}{2}\left(\frac{1}{T_1}-\frac{1}{T_{10}}\right)\right]/[Gd(dpaa) \quad (4)$$

where T_1 and T_2 are the experimental CH_3OD proton relaxation times in the solution containing the $[Gd(dpaa)(D_2O)_3]$ complex at the concentration [Gd(dpaa)], whereas T_{10} and T_{20} are the measured values in the absence of the complex. From the experimental values of Table 5, we obtain $r_{mix,m}^{OS}(\infty)=3.74$ s^{-1} mM^{-1}.

Now, turn to the interpretation of the HOD relaxivities. The total longitudinal and transverse relaxivities $r_{1,w}=11.93$ and $r_{2,w}=14.28$ s^{-1} mM^{-1} are readily obtained by substituting the measured values for the relaxation times T_1, T_2, T_{10} and T_{20} of the HOD protons in Equations (5a and b):

$$r_{1,w}=\left(\frac{1}{T_1}-\frac{1}{T_{10}}\right)/[Gd(dpaa)] \quad (5a)$$

$$r_{2,w}=\left(\frac{1}{T_2}-\frac{1}{T_{20}}\right)/[Gd(dpaa)] \quad (5b)$$

The purpose of the following steps of the relaxivity analysis is to disentangle the IS and OS contributions to the total relaxivities $r_{1,w}$ and $r_{2,w}$ to allow a straightforward estimation of their underlying geometric and dynamic molecular factors.

In step 2 the mixed relaxivity $r_{mix,w}^{OS}(\infty)$ of the HOD protons is calculated from Equation (6) [which is Eq. (25) from the Theory Section] when L = dpaa:

$$r_{mix,w}^{OS}(\infty)=r_{mix,w}^{OS}(\infty)\frac{D_{m/Gd(dtpaa)}}{D_{w/Gd(dtpaa)}}\frac{b_{m/Gd(dtpaa)}}{b_{w/Gd(dtpaa)}} \quad (6)$$

where $D_{X/Gd(dtpaa)}$ and $b_{X/Gd(dtpaa)}$ are the relative diffusion coefficient and the collision diameter of the X/Gd(dpaa) pair, respectively (X = methanol (m) or water (w)). The relative diffusion coefficient $D_{X/Gd(dtpaa)}$ is the sum given by Equation (7) of the self-diffusion coefficient D_X^t of the molecule X and of the self-diffusion coefficient $D_{Gd(dtpaa)}^t$ of the Gd^{III} complex.

$$D_{X/Gd(dtpaa)}=D_X^t+D_{Gd(dtpaa)}^t \quad (7)$$

The self-diffusion coefficients of the uncharged CH_3OD and HOD molecules are independent of the presence of dilute small solutes and have infinite dilution values that can be measured by the pulsed-gradient spin-echo (PGSE) NMR technique,[52] namely, these values are $D_m^t=1.13\times10^{-5}$ and $D_w^t=1.85\times10^{-5}$ cm^2s^{-1} in D_2O at 298 K. Three different procedures can be used to obtain the relative diffusion coefficients $D_{m/Gd(dtpaa)}$ and $D_{w/Gd(dtpaa)}$ involved in Equation (6). In procedure 1, the self-diffusion coefficient $D_{Gd(dtpaa)}^t$ of the $[Gd(dpaa)(D_2O)_3]$ complex is approximated by that of its Lu^{III} or La^{III} analogue, which is measured[25,53,54] by the PGSE NMR technique. Then, the relative diffusion coefficients are calculated as the sum of D_X^t and $D_{Gd(dtpaa)}^t$ [Eq. (7)]. As a goal of this study is to provide an economical determination of the factors that affect the relaxivity, procedure 1 is not used herein because the accompanying addi-

tional experimental work is not justified by the need of a precise measurement of $D^{t}_{Gd(dtpaa)}$, as discussed hereafter. Procedure 2 rests on an a priori estimation of the self-diffusion coefficient $D^{t}_{Gd(dtpaa)}$. The studied complex [Gd(dpaa)-$(D_2O)_3$] is a small Gd–polyaminocarboxylate complex (M_r= 500–750 g mol^{-1}). The self-diffusion coefficients of many complexes of this type were found to be in the range[54] $(0.45\pm0.1)\times10^{-5}$ cm^2 s^{-1} in H_2O at 298 K. According to the Stokes–Einstein law, the corresponding self-diffusion coefficients in D_2O should decrease by the viscosity ratio $\eta(D_2O)/\eta(H_2O)=1.24$ to take the value $(0.36\pm0.08)\times10^{-5}$ cm^2 s^{-1}. In procedure 2, the self-diffusion coefficient $D^{t}_{Gd(dtpaa)}$ of [Gd(dpaa)$(D_2O)_3$] in D_2O is simply assumed to have the mean value 0.36×10^{-5} cm^2 s^{-1}. As in procedure 1, the relative diffusion coefficients are calculated as the sum of D^{t}_{X} and $D^{t}_{Gd(dtpaa)}$ [Eq. (7)]. For its present use in Equation (6), the rough approximation of the self-diffusion coefficient $D^{t}_{Gd(dtpaa)}$ of [Gd(dpaa)$(D_2O)_3$] by an experimental mean value for the complexes of this type is sufficiently accurate. Indeed, given the reported self-diffusion coefficients of CH_3OD and HOD, the typical absolute uncertainty of $\pm0.08\times10^{-5}$ cm^2 s^{-1} of $D^{t}_{Gd(dtpaa)}$ gives a negligible relative uncertainty of less than 2% for the ratio $D_{m/Gd(dtpaa)}/D_{w/Gd(dtpaa)}$ appearing in Equation (6). In procedure 3, the relative diffusion coefficients $D_{m/Gd(dtpaa)}$ and $D_{w/Gd(dtpaa)}$ are estimated from the measured relaxivities without additional experimental work: First, the relative diffusion coefficient $D_{m/Gd(dtpaa)}$ is obtained from the values of $r^{OS}_{1,m}(\infty)=(1/T_1-1/T_{10})/[Gd(dpaa)]$ and $r^{OS}_{mix,m/Gd(dtpa)}$ given by Equation (4) by using Equation (8) [which is equivalent to Eq. (22) in the Theory Section]:

$$D_{m/Gd(dtpaa)}=\left[\frac{\lambda_D\sqrt{\pi\nu_I}}{r^{OS}_{mix,m}(\infty)-r^{OS}_{1,m}(\infty)}\right]^{2/3} \tag{8}$$

where the proton resonance frequency is $\nu_I=200\times10^6$ Hz. The m/[Gd(dpaa)$(D_2O)_3$] relative diffusion coefficient is $D_{m/Gd(dtpaa)}=1.55\times10^{-5}$ cm^2 s^{-1}. As discussed below, this value leads to a reasonable estimate of $D^{t}_{Gd(dtpaa)}$, so it is retained to calculate the mixed OS relaxivity of the HOD protons from Equation (6). Second, the w/Gd(dpaa) relative diffusion coefficient is obtained from Equation (9):

$$D_{w/Gd(dtpaa)}=D_{m/Gd(dtpaa)}+D^{t}_{w}-D^{t}_{m} \tag{9}$$

where $D_{w/Gd(dtpaa)}=2.27\times10^{-5}$ cm^2 s^{-1}. Finally, according to the previous subsection the collision diameters of the m/Gd-(dpaa) and w/Gd(dpaa) pairs estimated from compact molecular models are $b_{m/Gd(dtpa)}=6.1$ and $b_{w/Gd(dtpa)}=5.5$ Å. The mixed OS relaxivity ($r^{OS}_{mix,w}(\infty)=2.84$ s^{-1} mM^{-1}) of the HOD protons is now readily computed from Equation (6). Again, it should be emphasised that errors in the estimates of the radius and self-diffusion coefficients of a Gd–L complex cancel out to a large extent in the ratios $b_{m/GdL}/b_{w/GdL}$ and $D_{m/GdL}/D_{w/GdL}$, so that the determination of $r^{OS}_{mix,w}$ from $r^{OS}_{mix,m}$ should be accurate.

Though it is not necessary for the present analysis, the self-diffusion coefficient $D^{t}_{Gd(dtpaa)}$ of [Gd(dpaa)$(H_2O)_3$] can be readily estimated from the relaxivity measurements as follows: From the use of the retained value $D_{m/Gd(dtpaa)}=1.55\times10^{-5}$ cm^2 s^{-1} of the m/Gd(dpaa) relative diffusion coefficient, we have $D^{t}_{Gd(dtpaa)}=D_{m/Gd(dtpaa)}-D^{t}_{m}=0.42\times10^{-5}$ cm^2 s^{-1}. This result is in satisfactory agreement with the value $(0.36\pm0.08)\times10^{-5}$ cm^2 s^{-1} previously derived from the self-diffusion coefficients in solutions of gadolinium complexes of sizes similar to that of the studied complex in light water.[54]) However, note that the $D_{m/Gd(dtpaa)}$ value was calculated from the difference $r_{mix}(\infty)-r_1$, which has a large percentage error, because $r_{mix}(\infty)$ and r_1 have near values, as the $D_{m/Gd(dtpaa)}$ value is rather large and the ν_1 value is rather small. Then, the accuracy of the $D_{Gd(dtpaa)}$ value is not better than 30%. An improved accuracy could be obtained either from a relaxation study at a higher frequency or by replacing CH_3OD with another probe solute, such as *tert*-butanol(OD) of slower self-diffusion.

Step 3 is an application of Equation (22) to the determination of the OS relaxivities of the HOD protons. In this case, Equations (22a and b) can be rewritten as Equations (10a and b):

$$r^{OS}_{1,w}=r^{OS}_{mix,w}(\infty)-(\lambda_D/D^{3/2}_{w/Gd(dtpa)})\sqrt{\pi\nu_I} \tag{10a}$$

$$r^{OS}_{2,w}=\frac{7}{6}r^{OS}_{mix,w}(\infty)-\frac{1}{2}(\lambda_D/D^{3/2}_{w/Gd(dtpa)})\sqrt{\pi\nu_I} \tag{10b}$$

The relaxivities $r^{OS}_{1,w}=2.53$ and $r^{OS}_{2,w}=3.16$ s^{-1} mM^{-1} of the HOD protons are calculated from the previous determinations of the mixed relaxivity $r^{OS}_{mix,w}(\infty)=2.84$ s^{-1} mM^{-1} and the relative diffusion coefficient $D_{w/Gd(dtpaa)}=2.27\times10^{-5}$ cm^2 s^{-1}.

In step 4, the experimental IS relaxivities are obtained from the measured relaxation times T_1, T_2, T_{10} and T_{20} of the HOD protons by using Equations (11) [which is equivalent to Equation (17)]:

$$r^{IS}_{1,w}=r_{1,w}-r^{OS}_{1,w} \tag{11a}$$

$$r^{IS}_{2,w}=r_{2,w}-r^{OS}_{2,w} \tag{11b}$$

The values $r^{IS}_{1,w}=9.40$ and $r^{IS}_{2,w}=11.12$ s^{-1} mM^{-1} stem readily from Equation (11).

Finally, step 5 is the evaluation of the geometric and dynamic factors that are at the origin of the water-proton high-field relaxivity and have not yet been determined. To begin with, consider the IS relaxivity values of the HOD proton, which are well reproduced to within a few percent by their theoretical counterparts derived from the standard Equations (18)–(20), with a rotational correlation time $\tau_{R,Gd(dtpaa)}=103$ ps, a coordination lifetime $\tau_{M,Gd(dtpaa)}=0.1$ μs and a number of coordinated water molecules $q_{Gd(dpaa)}=3$, in agreement with the value measured independently by luminescence studies for the europium centre in terbium com-

plexes. The theoretical results are summarised in Table 6. Note that the uncertainty of the rotational correlation time can be mainly ascribed to that of the probable value[55] $r_H =$ 3.1 Å of the Gd–proton distance. It is also useful to estimate the precision of the method for evaluating the lifetime τ_M in the case of $[Gd(dpaa)(H_2O)_3]$, which is particularly unfavourable because τ_M is significantly shorter than $T_{1M} \cong T_{2M} \cong 5$ μs, so that its variation weakly affects the r_1^{IS} and r_2^{IS} theoretical values given by Equation (18). The experimental precision of T_1 is typically 0.5–1 % and that of T_2 or $T_{1,p}$ is 1–1.5 %. Simple inspection of the equations that lead to the estimates of the r_1^{IS} and r_2^{IS} values shows that their cumulative errors are about 2 and 3 %, respectively. The τ_M values inserted in Equation (18), which give theoretical relaxivities r_1^{IS} and r_2^{IS} compatible with their experimental counterparts to within the previous percentage errors of 2 and 3 %, lie in the range $0 \cong \tau_M \cong 0.23$ μs, namely, $\tau_M \cong 0.1 \pm 0.1$ μs. Thus, the exchange (ex) rate $k_{ex} = 1/\tau_M$ of the coordinated water molecules is at least rather fast. The value $\tau_M =$ 0.23 μs seems an upper limit beyond which the theoretical predictions do not agree with the experimental values of r_1^{IS} and r_2^{IS}. On the other hand, a very short coordination lifetime down to $\tau_M = 0.01$ μs should not be completely ruled out, even if the range of τ_M values $0.05 \cong \tau_M \cong 0.15$ μs, for which the theoretical relaxivities r_1^{IS} and r_2^{IS} are equal to the experimental values given in Table 6 to within 1 and 1.5 %, respectively, is more reasonable. It is worth noting that a preliminary interpretation of ^{17}O NMR spectroscopic measurements in light water[56] leads to a τ_M value shorter than 0.1 μs, in agreement with the present discussion. In further work, the accuracy of the present route to τ_M determination will be compared to the accuracy of the well-established ^{17}O NMR spectroscopic method[56,57] for several Gd^{III} complexes.

The longitudinal water proton relaxivity $r_{1,w}(H_2O) =$ 9.62 s^{-1} mM^{-1} that arises from the tris(aquo) complex $[Gd(dpaa)(H_2O)_3]$ in H_2O can be estimated by dividing the D_2O value reported in Table 6 by the viscosity ratio $\eta(D_2O)/\eta(H_2O) = 1.24$. It is approximately 2.5 times higher than that of most of the currently used commercial contrast agents. This high relaxivity is associated with the presence of three IS water molecules. A lower relaxivity ($r_1 = 7.15$ s^{-1} mM^{-1} at 20 MHz and 313 K) was measured for the tris(aquo) complex $[Gd(edta)]^-$ in H_2O.[58] The relaxivity as a result of the $[Gd(dpaa)(D_2O)_3]$ complex is constant between pD = 5.5 and 7.7 ($r_1 \cong 11.8$ s^{-1} mM^{-1} in D_2O at 200 MHz), whereas a lower value of $r_1 \cong 9.30$ s^{-1} mM^{-1} is measured at a basic pD value (11.6), in agreement with the presence of hydroxo species at this pD value with only two Gd^{III}-bound water molecules.

The analysis of the relaxivities for the $[Gd(dpaa)_2(D_2O)]^{3-}$ complex, also denoted by $Gd(dpaa)_2$, is similar to that carried out for $[Gd(dpaa)(D_2O)_3]$. In addition, two simplifying hypotheses are made: 1) The volume of $Gd(dpaa)_2$ is twice that of Gd(dpaa), so that the radius of $Gd(dpaa)_2$ is 5.1 Å, as mentioned previously. 2) The standard Stokes–Einstein laws of translational and rotational diffusion of large species are valid so that the self-diffusion coefficient $D^t_{Gd(dtpaa)_2} = 0.33 \times 10^{-5}$ $cm^2 s^{-1}$ of $Gd(dpaa)_2$ is that of Gd(dpaa) divided by $2^{1/3}$ and its rotational correlation time $\tau_{R,Gd(dtpaa)_2} = 206$ ps is twice that of Gd(dpaa). The experimental mixed OS relaxivity $r^{OS}_{mix,m} = 3.12$ of the CH_3OD protons is derived from the measured relaxation times with the help of Equation (23) or (4) adapted for $Gd(dpaa)_2$. The relaxivities $r^{OS}_{1,m}$, $r^{OS}_{2,m}$ or $r^{OS}_{1,\rho,m}$ obtained from the definition given by Equation (15) satisfy Equation (22) with the mixed relaxivity and the relative diffusion coefficient of the pair to within the experimental errors. Then, the experimental mixed OS relaxivity $r^{OS}_{mix,w}$ of the HOD proton is obtained by applying Equation (6) adapted for $Gd(dpaa)_2$. The OS relaxivities $r^{OS}_{1,w}$ and $r^{OS}_{2,w}$ of the HOD protons are given by Equation (22) or (10) adapted for $Gd(dpaa)_2$. The total relaxivities $r_{1,w}$ and $r_{2,w}$ are obtained from their definition given by Equation (15). The IS relaxivities $r^{IS}_{1,w}$ and $r^{IS}_{2,w}$ follow from Equations (17) or (11). They can be interpreted by the standard IS relaxation model of Equations (18)–(20) with $\tau_{R,Gd(dtpaa)_2} = 206$ ps, a coordination lifetime of $\tau_{M,Gd(dtpaa)_2} = 0.45$ μs and a number of coordinated water molecules $q_{Gd(dpaa)_2} = 1$. This number of water molecules is in agreement with the value measured by luminescence for the terbium complex (Table 6). The coordination lifetime $\tau_M = 0.1$ μs is reasonable for $[Gd(dpaa)(H_2O)_3]$ as a ligand-like $dpaa^{3-}$ allows rather large free access of the Gd^{III} ion to the water molecules. When the Gd^{III} centre in $[Gd(dpaa)_2(H_2O)]^{3-}$ is complexed by two ligands, there is less free access and the τ_M value increases to 0.45 μs.

The rotational correlation times derived from the previous analysis are for the complexes in D_2O. Their counterparts in H_2O should be shorter by the factor $\eta(D_2O)/\eta(H_2O) = 1.24$. They are expected to be 83 and 166 ps for $[Gd(dpaa)(H_2O)_3]$ and $[Gd(dpaa)_2(H_2O)]^{3-}$, which are typical values for complexes of these sizes.[23,59] Finally, the determination of the OS relaxivities is model independent. In particular, it is applicable to Gd–L complexes that have anisotropic shapes and/or off-centre positions of the Gd^{III} centre, and for which the standard Ayant–Belorizky–Hwang–Freed (ABHF) OS relaxation model,[60,61] which involves two spins located at the centres of diffusing hard spheres, becomes questionable.

Interactions of $[Gd(dpaa)(D_2O)_3]$ with oxyanions: The quite high relaxivity observed for these complexes prompted us to investigate the effect of physiological anions on the relaxivity of $[Gd(dpaa)(D_2O)_3]$ to evaluate the behaviour in vivo and the potential for application.

Physiological anions can displace the ligand, thus resulting in insoluble adducts and toxicity,[62] or they can replace the water molecules coordinated to the gadolinium centre to form ternary adducts and therefore decrease the contrast efficiency of the complex. It has been observed previously that the presence of phosphate species dramatically decreases the relaxivity of gadolinium complexes of hexadentate texaphyrins from 17 to 5 s^{-1} mM^{-1}.[16] In the $do3a^{3-}$ derivatives, both IS water molecules are replaced by bidentate

anions, such as malonate and lactate species, whereas only one water molecule is displaced by a carbonate or phosphate moiety.[14,63,64]

The introduction of carboxylate groups on the do3a^{3-} ligand prevents anion and protein binding,[17] whereas the relaxivity of the bis(aquo) gadolinium complexes of a tripodal hydroxypyridone-based ligand is decreased significantly by only two physiological anions, phosphate and oxalate, the other anions, including citrate, have negligible effects.[20] It is evident from these data that anion binding is very sensitive to the charge of the complex and minor variations in the ligand structure and geometry.[11] However, there is still a lack of clear understanding of the dependency of anion binding from the structural properties.

The three metal-bound water molecules in the [Gd(dpaa)-$(D_2O)_3$] complex can be partially or totally replaced by oxyanions, which coordinate to the Gd^{III} centre to form ternary complexes with [Gd(dpaa)$(H_2O)_3$]. As the IS contribution to the relaxivity is proportional to the mean number $\bar{q}$ of metal-bound water molecules, the drop in the measured relaxivity, when adding an oxyanion, is directly proportional to the number of replaced water molecules and can be used to study the coordination of the metal centre by the oxyanion. The interaction of several physiological anions with [Gd(dpaa)$(D_2O)_3$] was studied by relaxometric analysis to investigate the influence of the ligand geometry on the formation of ternary adducts. The values of relaxivity measured for the neutral complex [Gd(dpaa)$(D_2O)_3$] in presence of a 200-fold excess of six different physiological anions are reported in Table 7.

Table 7. Longitudinal relaxivity r_1 and relaxivity difference $\Delta r_1 = r_{1\text{without anion}} - r_{1\text{with anion}}$ for [Gd(dpaa)$(H_2O)_3$] in the presence of 200 equivalents of various physiological anions.[a]

Anion	r_1 [s^{-1} mM^{-1}]	Δr_1 [s^{-1} mM^{-1}]
–	11.64	–
acetate	9.19	−2.45
lactate	8.24	−3.4
biphosphate	7.75	−3.89
bicarbonate	6.30	−5.34
oxalate	6.15	−5.49
citrate	2.87	−8.77

[a] Experimental conditions: 200 MHz, D_2O, pD ≈ 7.4, [Gd(dpaa)] ≈ 3 mM, [physiological anions] ≈ 600 mM.

The relaxivity decreases significantly for all anions, thus indicating that anion binding occurs. The observed values can be roughly interpreted as follows, with the help of the relaxivity analysis of the free [Gd(dpaa)$(D_2O)_3$] complex presented previously. The experimental OS relaxivity is $r_{1,w}^{OS} = 2.53\ s^{-1}\ mM^{-1}$ for the HOD proton, and the IS contribution per coordinated water molecule is $r_{1,w}^{IS}/3 = 3.13\ s^{-1}\ mM^{-1}$. As the oxyanions that replace the metal-bound water molecules are small species with respect to the Gd(dpaa) complex, both the OS and IS dynamics of the ternary complexes should be similar to those of the free complex. Then, the predicted relaxivity for ternary complexes with $q^{(b)}$ ((b) = bound) metal-bound water molecules should be approximately $r_1^{adduct}(q^{(b)}) = 2.53 + q^{(b)} \times 3.13\ s^{-1}\ mM^{-1}$, that is, 2.5, 5.7 and 8.8 $s^{-1}\ mM^{-1}$ for $q^{(b)} = 0$, 1 and 2, respectively. This suggests that all the three metal-bound water molecules of [Gd(dpaa)$(D_2O)_3$] are replaced by citrate, two of them by bicarbonate and oxalate, and only one by acetate, biphosphate and lactate in the presence of a 200-fold excess of anions with respect to the free complex. Even under these conditions that are favourable to the formation of adducts with oxyanions, the mean relaxivity remains higher than those of most of the currently used commercial contrast agents except for the citrate. However, the measured relaxivity $\bar{r}_1 = 7.9\ s^{-1}\ mM^{-1}$ in a solution containing equimolar concentrations of [Gd(dpaa)$(H_2O)_3$] and citrate is still high.

The formation constant K_{adduct} of a ternary adduct with an oxyanion can be derived from the variation of the mean relaxivity of the HOD proton versus the oxyanion concentration by using Equation (33) (see the Theory Section). The relaxivity $\bar{r}_1$ was measured at different concentrations of the citrate and bicarbonate anions (see the Supporting Information), which are present in the blood plasma at concentrations[65] (0.06–0.16 and 22–28 mM for citrate and bicarbonate, respectively) comparable to that of a contrast agent distributed in the extra-cellular fluid after administration of a standard dose of 0.1 mmol kg^{-1} body weight.[66] The fitting of the relaxivity data reported in the Supporting Information provides satisfactory adduct relaxivities and formation constants ($r_1^{(b)} = 2.7\ s^{-1}\ mM^{-1}$, $\log K_{adduct} \cong 3.7$ for citrate at pD = 7.6 and $r_1^{(b)} = 5.35\ s^{-1}\ mM^{-1}$, $\log K_{adduct} \cong 1.8$ for bicarbonate at pD = 7.4).

Thus, the high relaxivity of the gadolinium complex of this tripodal tris(picolinate) ligand is only partially decreased by most of the physiological anions in spite of the neutral charge of the complex. Analogous ligands that lead to negatively charged complexes should lead to improved stability and lower affinity for physiological anions. Studies in this direction are in progress. A comparison with the results reported for the interaction with physiological anions for the tripodal hopo derivatives tren-bis-hopo-tam ligands[20,67] reveals an increased interaction with some physiological anions. This behaviour could be explained by the higher number of IS water molecules that result in higher accessibility of the coordination sites for anion binding or by an overall different geometry in solution. The investigation of anion binding by bis(aquo) or tris(aquo) gadolinium complexes with picolinate ligands with different architectures should give more insight into the relation between ligand geometry and the displacement by physiological anions of water molecules bound to gadolinium.

Interactions of [Gd(dpaa)$(H_2O)_3$] with bovine serum albumin (BSA): For most of the clinical imaging fields, which range from 0.5 to 1.5 T, it is well known that slowing down the Brownian rotation of a Gd–L complex by covalent or noncovalent interactions with a macromolecular solute is an efficient way to increase the IS contribution to the relaxivity provided that the residence time τ_M of a metal-bound water

molecule is on the order of 0.1 μs or shorter.[7,66] In the case of blood-pool contrast agents, this process can be achieved by noncovalent binding of mono(aquo)–gadolinium complexes to the abundant plasma protein, serum albumin.[68–72] Unfortunately, the side-chain carboxylate groups of the proteins, such as serum albumin, may cause a partial or total displacement of the coordinated water molecules of the bis- and tris(aquo) complexes, thus suppressing the relaxivity enhancement benefit as a result of the high number of these water molecules in the free complex.[9,10,66,73] The presence of hydrophobic pyridine groups on the dpaa ligand incited us to explore whether $[Gd(dpaa)(H_2O)_3]$ binds to a plasma albumin, such as BSA, of molecular weight $M_{BSA}=66\,400$ Da, and if the final adduct retains the IS water molecules of the free complex upon binding. To investigate the interaction of the protein with the $[Gd(dpaa)(H_2O)_3]$ complex and, in particular, its effect on the coordination environment of the gadolinium centre, we performed luminescence studies in the presence of BSA[74] and measured the water-proton longitudinal and transverse relaxivities in solutions of the gadolinium complex containing increasing BSA concentrations at 298 K and a proton resonance frequency of 60 MHz that correspond approximately to the imaging field of 1.5 T.

The observed luminescence lifetimes of the $Tb(^5D_4)$ (τ_{H_2O} $t=1.04(3)$ ms and $\tau_{D_2O}=1.63(2)$ ms) levels for a solution of [Tb(dpaa)] (4 mM) with BSA (12% w/v) are in agreement with the presence of a mean number $\bar{q}=1.54\pm0.2$ of metal-bound water molecules. The decrease in the observed number of metal-bound water molecules from $q^{(f)}=3.1\pm0.2$ in the absence of BSA to $\bar{q}=1.54\pm0.2$ in presence of this protein requires the existence of BSA binding sites, for which the number of water molecules coordinated to the Gd^{III} centre is decreased to 1 or 0 [according to Eq. (32) of the Theory section]. Assuming that all the n_{BSA} BSA binding sites of $[Gd(dpaa)(H_2O)_3]$ are equivalent, the number of water molecules coordinated to the Gd^{III} centre, when the complex is bound to BSA, has to be $q^{(b)}=q_{BSA}=1$ or 0. First, consider the situation $q_{BSA}=1$, which would imply the coordination of the protein side-chain carboxylate groups to the gadolinium centre in a bi- or monodentate fashion.[17] The number n_{BSA} of binding sites and the association constant k per site are unknown and will now be inferred from r_1 and r_2 measurements in solutions of $[Gd(dpaa)(H_2O)_3]$ of various BSA concentrations. The compositions of the studied solutions and relaxivity values are reported in the Supporting Information. The theoretical expressions given by Equation (33) of the mean relaxivities $\bar{r}_1$ and $\bar{r}_2$, derived in the Theory section, with the equilibrium concentration $[C]_{eq}$ of the free complex given by Equation (31), were fitted to their experimental counterparts. The theoretical mean relaxivities $\bar{r}_1$ and $\bar{r}_2$ are displayed in Figure 6 for selected values of $n_{BSA}=2$, 4, 10 and 20 and associated formation constants per site $k=1300$, 360, 110 and 50 $L\,mol^{-1}$, which are compatible with the experimental value of $\bar{q}$. The agreement with experiment improves significantly with an increasing number of binding sites and reaches a plateau for $n_{BSA}\geq10$,

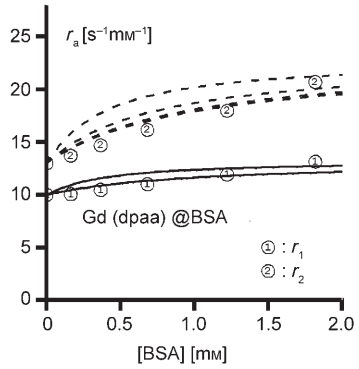

Figure 6. Longitudinal and transverse relaxivities r_1 and r_2 of the H_2O protons at 60 MHz as a result of the complex $[Gd(dpaa)(H_2O)_3]$ as a function of the concentration of BSA at 298 K. The mean relaxivities $\bar{r}_1$ and $\bar{r}_2$ given by Equation (33) are represented by continuous (top: $n=2$ and 4, bottom: $n=10$ and 20) and dashed curves (from the top: $n=2$ and 4; overlapping curves: $n=10$ and 20) respectively. These values tend to the experimental values as the number of BSA binding sites n increases.

in which case the association constant k is on the order of 100 or smaller, in accordance with the formation constants of the Gd(dpaa) adducts with mono- and bidentate oxyanions. It should be emphasised that the limiting relaxivities $r_1^{(b)}=r_{1,BSA}=13.2$ and $r_2^{(b)}=r_{2,BSA}=22.8\,s^{-1}\,mM^{-1}$ at 60 MHz of the bound Gd(dpaa) complex used in the fitting procedure were not adjusted. These values were simply taken to be the sums of the OS values for the free $[Gd(dpaa)(H_2O)_3]$ complex in H_2O derived from experiment as shown previously and of the IS values obtained from the SBM Equations (18)–(20) with $\tau_R=9.3$ ns and $\tau_M=0.8$ μs. As suggested by Bertini et al.,[75] the rotational correlation time was obtained from the standard equation $\tau_R=\eta M_{BSA}/(dRT)$, where η is the H_2O viscosity and $d=1\,g\,cm^{-3}$ the density of BSA. Its value is similar to those proposed by Caravan et al.[70] The coordination lifetime τ_M was the only fitted parameter in addition to the number of binding sites. This lifetime has a reasonable value, longer than that of $[Gd(dpaa)(H_2O)_3]$ because of the binding site of BSA and is similar to that of $[Gd(dpaa)_2(H_2O)]^{3-}$. To be complete it should be pointed out that the effects of the electronic spin longitudinal relaxation of the Gd^{III} ion on the $r_{1,BSA}$ and $r_{2,BSA}$ values may not be completely negligible at 60 MHz, even though it is due to the sole fluctuations of the so-called transient zero-field splitting (ZFS) Hamiltonian.[76]

Indeed, assuming that the transient ZFS Hamiltonian of $[Gd(dpaa)_2(H_2O)]^{3-}$ has the typical parameters of the $[Gd(dota)(H_2O)]^-$ complex,[59] the longitudinal electronic relaxation time T_{1e} is only slightly longer than the rotational correlation time of BSA, and thus will modify the relaxivities $r_{1,BSA}$ and $r_{2,BSA}$ of the bound Gd(dpaa) complex. We checked that such a modification does not significantly alter the conclusion of the present BSA study. A more precise theory would require not only a reliable characterisation of the transient ZFS Hamiltonian, but also a description of the OS relaxivities, thus accounting for the location of the bound complexes at the BSA surface. This investigation is

far beyond the purpose of this study. Also note that because of the mass-action laws the concentration of bound Gd(dpaa) is larger for a number of $2n_{BSA}$ binding sites of association constant $k/2$ than for n_{BSA} binding sites of the association constant k. To sum up, to interpret the luminescence and relaxivity data in the case of $q_{BSA}=1$, it was possible to build a simple binding model of Gd(dpaa) and BSA depending on structural and dynamic parameters, which were derived from simple physical considerations or obtained by elementary mathematical treatment without multiparameter fitting.

Turn to the second situation of $q_{BSA}=0$, which is compatible with the experimental average number of metal-bound water molecules $\bar{q}=1.54\pm0.2$. A purely OS relaxation mechanism leads to theoretical relaxivities that are much smaller than the values measured in the presence of BSA. Therefore, a second-sphere (2S) relaxation mechanism[7,66,77] has to be invoked. The coordination lifetime τ_M to be fitted in the case of $q_{BSA}=1$ is replaced by its counterpart τ'_M for 2S water molecules, the number q' and the distances r'_H to the Gd^{III} centre, which are unknown and have also to be fitted. The longitudinal and transverse 2S relaxivities $r^{2S}_{1,BSA}$ and $r^{2S}_{2,BSA}$ are given by[7] Equation (12):

$$r_\alpha^{2S}=\frac{Pq\prime}{T'_{\alpha M}+\tau'_M} \tag{12}$$

where the intramolecular relaxation rates $1/T_{1M}'$ and $1/T_{2M}'$ are expressed in terms of the 2S spectral density $j^{2S}_{2c}(t\omega)$ as Equations (13a and b)

$$1/T'_{1M}=Aj^{2S}_{2c}(i\omega) \tag{13a}$$

$$1/T'_{2M}=A\left[\frac{2}{3}j^{2S}_{2c}(0)+\frac{1}{2}j^{2S}_{2c}(i\omega_I)\right] \tag{13b}$$

At high field, the spectral density $j^{2S}_{2c}(t\omega)$ is of the form given in Equation (14):

$$j^{2S}_{2c}(\tau=i\omega)=\frac{1}{4\pi r'^6_H}\frac{\tau\prime_c}{1+\omega^2\tau'^2_c}\ \text{with}\ \frac{1}{\tau'_c}\equiv\frac{1}{\tau_R}+\frac{1}{\tau'_M} \tag{14}$$

Equations (12)–(14) are formally identical to Equations (18)–(20), which describe the IS relaxivities, but the correlation time τ'_c of the 2S relaxation mechanism is much shorter than the correlation time τ_R of the IS relaxation mechanism. Indeed, the residence lifetime τ'_M is expected to be[78] less than 100 ps so that it is much shorter than τ_R and $\tau'_c\cong\tau'_M\ll\tau_R$. The consequence for the values of the 2S relaxivities $r^{2S}_{1,BSA}$ and $r^{2S}_{2,BSA}$ of the bound complex is that $r^{2S}_{2,BSA}$ exceeds $r^{2S}_{1,BSA}$ by less than 15%. This difference is transferred to the total relaxivities $r_{1,BSA}$ and $r_{2,BSA}$ of the bound complex so that $r_{2,BSA}$ exceeds $r_{1,BSA}$ only by a similarly small percentage. This theoretical property is incompatible with the experimental relaxivity values as, for example, the r_2^{exp} value is about 60% larger than the r_1^{exp} value at the highest BSA concentration! Briefly, the observed variation in relaxivities with BSA concentration cannot be explained by the standard model of 2S relaxivity with a reasonable residence lifetime τ'_M of the 2S water molecules.

According to these results the $[Gd(dpaa)(H_2O)_3]$ complex interacts with several equivalent sites of serum albumin with a binding constant similar to that found for the interaction of the complex with bidentate anions. This behaviour leads to the displacement of only two coordinated water molecules and to an overall increase of the final relaxivity of the gadolinium complex in the presence of serum albumin.

Finally it is worth discussing the limits of the previous analysis of the relaxivity observed for $[Gd(dpaa)(H_2O)_3]$ in the presence of BSA. From the above interpretation, it is clear that the interaction of this complex with BSA is quite complicated so that the various measured relaxometric properties are not sufficient, even for a preliminary investigation. For example, it would have been tempting to interpret the measured relaxivity values in terms of a high relaxivity of the complex bound to a single site of albumin with a low binding constant. However, this interpretation is not compatible with the measured number of coordinated water molecules by luminescence lifetime studies, and the interpretation of both experimental data requires the introduction of several binding sites with a higher affinity constant. The previous analysis also indicates that the combination of the relaxometric and spectrofluorimetric properties is still insufficient to discriminate between 4–20 binding sites. For that purpose, the isolation and characterisation of the albumin-bound species is needed.[70] Finally, a more precise description beyond the rough model presented herein would require measurement of the water-exchange rate. Studies in that direction are in progress.

Conclusion

The new hexadentate picolinate ligand $dpaa^{3-}$ forms a tris(aquo) gadolinium complex with high water solubility, reasonable stability at physiological pH and fairly high relaxivity at high field. At a pH value higher than 8, the formation of soluble hydroxo complexes is accompanied by a decrease in the relaxivity. The hydroxo and the aquo complexes self-assemble in the solid state through the formation of carboxylate bridges between different gadolinium centres and between gadolinium centres and sodium cations to build a rare 1D coordination polymer of square-shaped tetrameric units. A new versatile method to unravel the geometric and dynamic molecular factors that explain the high-field relaxivities has been developed. This method uses a small, uncharged non-coordinating probe solute, the OS relaxivity of which mimics that of the water proton; furthermore, only routine NMR spectrometric and simple mathematical analysis is required. In particular, numerical multiparameter fitting sometimes based on physically questionable assumptions is not needed.

The tris(aquo) complex interacts strongly with physiological anions, and the formation of ternary complexes is accom-

panied by a significant decrease in the relaxivity value. Nevertheless, the relaxivity of the ternary complex remains high in most cases, and low relaxivity values are only observed in the presence of a 200-fold excess of citrate. The selective interaction with biological dianions, which leads to significant variation of the relaxivity, is of particular interest because of the potential application in monitoring the concentration of metabolites in clinical examinations. The affinity of this gadolinium complex for biological anions and the observed changes in relaxivity upon anion binding are strongly dependent on the anion structure and differ significantly from the observations of other tris- and bis(aqua) complexes previously reported. The interaction of the tris(aqua) complex with the protein bovine serum albumin displaces only two of the three coordinated water molecules so that the exchangeable remaining water molecule can still yield a small relaxivity enhancement as the protein concentration increases. All these results show the importance of structural variation on the formation of ternary complexes and the need for more systematic studies. The objective is to control ternary complex formation by ligand design either to prevent it or to favour selective interaction.

Experimental Section

General: ^{1}H NMR spectra were recorded at 400 MHz on a Varian Unity 400 spectrometer and at 200 MHz on an Avance DMX 200 Brucker spectrometer. Chemical shifts are reported in ppm with the solvent as the internal reference. Mass spectra were obtained with a Finnigan LCQ-ion trap equipped with an electrospray source. Elemental analyses were performed by the Service Central d'Analyse (Vernaison, France).

Solvents and starting materials were obtained from Aldrich, Fluka, Acros and Alfa and used without further purification. Anhydrous acetonitrile was purchased from Aldrich and used without further purification. 6-Chloromethylpyridine-2-carboxylic acid ethyl ester was obtained from the commercially available 2,6-dipicolinic acid according to a published procedure.[79] BSA fraction V (99%) was purchased from Aldrich.

Synthesis of the ligand H_3dpaa

***N,N′*-Bis[(6-carbethoxypyridin-2-yl)methyl]glycyl ethyl ester:** 6-Chloromethylpyridine-2-carboxylic acid ethyl ester (0.582 g, 2.93 mmol), K_2CO_3 (0.618 g, 4.37 mmol) and KI (0.488 g, 2.91 mmol) were successively added to a solution of glycine ethyl ester hydrochloride (0.169 g, 1.21 mmol) in anhydrous acetonitrile (20 mL). The reaction mixture was stirred at room temperature for 1 h and then heated at 60 °C for 2 days. After filtration and evaporation of the solvent, the resulting crude product was dissolved into $CHCl_3$ (100 mL) and washed with a semi-saturated solution of $NaHCO_3$. After extraction of the aqueous layer with $CHCl_3$ (2×50 mL), the organic layer was dried over Na_2SO_4, filtered and evaporated to dryness. Further purification of the crude product by column chromatography on alumina activity III (75 mL; CH_2Cl_2/EtOH 100:1→95:5) yielded the desired product as a yellow solid (0.301 g, 58%). ^{1}H NMR (200 MHz,$CDCl_3$, 298 K): δ=1.26 (t, J=7.2 Hz, 3H, $COOCH_2CH_3$), 1.43 (t, J=7.2 Hz, 6H, py$COOCH_2CH_3$), 3.47 (s, 2H, CH_2COOEt), 4.08 (s, 4H, CH_2py), 4.16 (q, J=7.2 Hz, 2H, $COOCH_2CH_3$), 4.46 (q, 4H, J=7.2 Hz, py$COOCH_2CH_3$), 7.83 (m, 4H, CH), 8.01 (t, J=4.8 Hz, 2H, CH) ppm; ES-MS: *m/z* (%): 452.3 (100) $[M+Na]^+$, 430.3 (15) $[M+H]^+$.

***N,N′*-Bis[(6-carboxypyridin-2-yl)methyl]glycine (H_3dpaa)**: The synthetic strategy used for the formation of H_3dpaa is shown in Scheme 2. *N,N′*-Bis[(6-carbethoxypyridin-2-yl)methyl]glycyl ethyl ester (0.270 g, 0.63 mmol) was heated to reflux overnight in a 6 M HCl aqueous solution (40 mL). After evaporation of the solvent (≈3 mL) and cooling the resulting solution at 4 °C overnight, a white solid was formed by precipitation and collected by filtration, washed with Et_2O and dried under vacuum to yield H_3dpaa·1HCl·0.1H_2O (0.142 g, 65%). ^{1}H NMR (400 MHz, D_2O, 298 K, pD=4.7): δ=3.94 (s, 2H, H_1), 4.60 (s, 4H, H_2), 7.43 (d, J=7.6 Hz, 2H, H_3), 7.76 (d, J=7.6 Hz, 2H, H_5), 7.76 (t, J=7.6 Hz, 2H, H_4) ppm; ES-MS: *m/z* (%): 346.1 (100) $[M+H]^+$; elemental analysis (%) calcd for $C_{16}H_{15}N_3O_6$·1HCl·0.1H_2O: C 50.10, H 4.26, N 10.96; found: C 50.15, H 4.31, N 10.91; the salt content was confirmed by potentiometric titration.

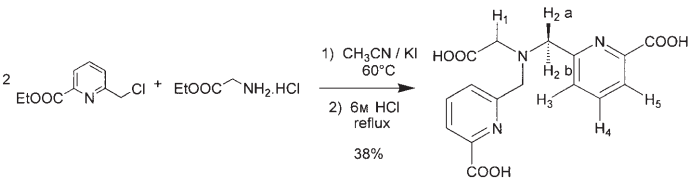

Scheme 2.

Synthesis of the lanthanides complexes

[Gd(dpaa)(H_2O)$_3$] (1): A solution of $GdCl_3$·6H_2O (0.17 mmol) in Milli-Q (mQ) ultrapure water (1 mL) was added to a solution of H_3dpaa (0.17 mmol) in water (2 mL). The pH value of the resulting mixture was adjusted to pH≈6 by adding an aqueous solution of NaOH (1 M). After evaporation of water, the resulting solid was suspended in ethanol (20 mL). The resulting suspension was stored at 4 °C overnight, and NaCl was eliminated by filtration. This operation was repeated several times until most of the salts had been eliminated. The resulting solution was taken to dryness and dissolved in mQ water (0.7 mL). Slow diffusion of acetonitrile (≈5 mL) at 4 °C yielded the [Gd(dpaa)(H_2O)$_3$] complex as a white microcrystalline solid (65%). ES-MS: *m/z* (%): 771.9 (30) $[[\{Gd(dpaa)\}_3]+2Na]^{2+}$, 1022.0 (100) $[[\{Gd(dpaa)\}_4]+2Na]^{2+}$, 1271.7 (30) $[[\{Gd(dpaa)\}_5]+2Na]^{2+}$, 1520.9 (30) $[[\{Gd(dpaa)\}_3]+Na]^{+}$; elemental analysis (%) calcd for [Gd(dpaa)]·0.8NaCl·5.8H_2O·0.2EtOH: C 29.85, H 3.79, N 6.37, Gd 23.83; found: C 29.96, H 3.79, N 6.39, Gd 23.53.

[{[Gd(dpaa)(H_2O)]$_2$[Gd(dpaa)(H_2O)(OH)]Na(H_2O)$_2$}$_2$]$_2$Na(OH)(H_2O)$_3$·CH_3OH·6H_2O]$^\infty$ (3): Obtained as crystals by slow evaporation of an ≈10^{-2} M solution of **1** after adjustment of the pH value to 8.

[Lu(dpaa)(H_2O)$_2$] (2): A solution of $LuCl_3$·6H_2O (0.048 mmol) in mQ water (1 mL) was added to a solution of H_3dpaa (0.048 mmol) in water (2 mL). The pH value of the resulting mixture was adjusted (pH 5.27) by adding an aqueous solution of KOH (1 M). The solution was evaporated to approximately 1 mL and stored at 4 °C. After a few days, white crystals formed. KCl was eliminated by washing with small aliquots of cold mQ water. The solid was dried to yield the [Lu(dpaa)(H_2O)$_2$] complex as a white microcrystalline solid (82%). Crystals suitable for X-ray diffraction were obtained by slow evaporation of a concentrated solution of the complex in water. Elemental analysis (%) calcd for [Lu(dpaa)]·0.7KCl·1.0H_2O·0.8EtOH: C 33.87, H 3.04, N 6.73; found: C 33.99, H 3.02, N 6.59.

The samples of the Ln(dpaa) (Ln=Lu, La, Eu) complexes for the NMR measurements were prepared by dissolving equimolar amounts of the ligand and the hydrate [Ln(OTf)$_3$] in D_2O followed by adjustment of the pD value with solutions of NaOD in D_2O. Concentrations in the range of 2×10^{-2}–5×10^{-2} M were used. The pH values given are corrected for deuterium isotope effects.[80]

[La(dpaa)(H_2O)$_x$]: ^{1}H NMR (D_2O, 400 MHz, 298 K, pD 8.1): δ=3.62 (s, 2H, H1), 4.13 (d, J=16 Hz, 2H, H2a/H2b), 4.26 (d, J=16 Hz, 2H, H2a/H2b), 7.61 (d, J=8 Hz, 2H, H3), 7.93 (d, J=8 Hz, 2H, H5), 8.03 ppm (t, J=8 Hz, 2H, H4).

[Lu(dpaa)(H_2O)$_2$]: ^{1}H NMR (D_2O, 400 MHz, 298 K, pD 6.7): δ=3.85 (s, 2H, H1), δ_A=4.46, δ_B=4.52 (dd, J_{AB}=15.4 Hz, 4H, H2a+H2b), 7.83 (d, J=7.6 Hz, 2H, H3), 8.10 (d, J=7.6 Hz, 2H, H5), 8.25 ppm (d, J=7.6 Hz, 2H, H4).

[Eu(dpaa)(H_2O)$_3$]: ^{1}H NMR (D_2O, 400 MHz, 298 K, pD 7.9): $\delta = -2.78$ (s, 2H, H1), 3.25 (s, 2H, H3/H5), 3.87 (s, 2H, H2a/H2b), 6.64 (s, 2H, H4), 7.50 (s, 2H, H3/H5), 10.76 ppm (s, 2H, H2a/H2b).

A 2D-COSY experiment performed at 298 K allowed the differentiation between the protons of the pyridine ring: cross peaks between H4/H2 and H4/H5 were observed.

Potentiometric titrations: Ligand-protonation and metal-ion stability constants with H_3dpaa were determined by potentiometric titrations. Solutions of Gd^{III} and Tb^{III} were prepared by dissolving the appropriate amounts of $GdCl_3 \cdot 6H_2O$ and $TbCl_3 \cdot 6H_2O$ (Aldrich) in water. The exact concentration of Ln^{3+} ions was determined by colourimetric titration in acetate buffer (pH 4.5) by using standardised H_2Na_2edta solutions (Aldrich) and xylenol orange as the indicators. Aliquots of 20-mL solutions of H_3dpaa ($7.5 \cdot 10^{-4}$ M) alone, acidified (pH $\approx$ 2.7) 1:1 Gd/ligand mixtures ([L] = $4.3 \cdot 10^{-4}$ M), acidified (pH $\approx$ 2.7) 1:2 Gd/ligand mixtures ([L] = $4.4 \cdot 10^{-4}$ M, [Gd] = $2.2 \cdot 10^{-4}$ M), acidified (pH $\approx$ 2.5) 1:1 Tb/ligand mixtures ([L] = $3.6 \cdot 10^{-4}$ M) and acidified (pH $\approx$ 2.7) 1:2 Tb/ligand mixtures ([L] = $1.8 \cdot 10^{-4}$ M, [Tb] = $3.6 \cdot 10^{-4}$ M) were titrated in a thermostated cell (25.0 $\pm$ 0.1 °C) under a stream of argon with a 0.1 M KOH solution added by means of a 5-mL piston burette (Metrohm). The ionic strength was fixed with KCl ($\mu = 0.1$ M). Titrations were carried out with a Metrohm 751 GPD Titrino potentiometer equipped with a combined pH glass electrode (Metrohm). Calibration of the electrode system was performed prior to each measurement. The electromotive force is given by $E = E° + s$ pH and both $E°$ and s were determined by titrating a known amount of HCl with 0.1 M KOH at $\mu = 0.1$ M (KCl) by using the acid range of the titration. The value used for the ion product of water is $\log K_w = 13.77$.[81] More than 58 data points were collected for each experiment.

The data were mathematically treated by the program HYPERQUAD2000.[82,83] All values and errors represent the average of at least three independent experiments.

X-ray crystallography: All the diffraction data were recorded on a Bruker SMART CCD area detector three-circle diffractometer ($Mo_{K\alpha}$ radiation, graphite monochromator, $\lambda = 0.71073$ Å). To prevent evaporation of co-crystallised water molecules, the crystals were coated with light hydrocarbon oil and the data were collected at −50 °C. The cell parameters were obtained with intensities detected on three batches of 15 frames with a 10-s exposure time for **3** and with all data collection for **2**. The crystal–detector distance was 5 cm. For three settings of Φ, 1271 narrow data frames for **3** and **2** were collected for 0.3° increments in ω with an exposure time for of 10 and 300 s for **3** and **2**, respectively. At the end of the data collection, the first 50 frames were recollected to establish that crystal decay had not taken place during the collection. Unique intensities with $I > 10\sigma(I)$ detected on all frames using the Bruker Saint program[84] were used to refine the values of the cell parameters. The substantial redundancy in the data allows empirical absorption corrections to be applied using multiple measurements of equivalent reflections with the SADABS Bruker program.[84] Space groups were determined from systematic absences, and they were confirmed by the successful solution of the structure (Table 1). Complete information on crystal data and data collection parameters is given in the Supporting Information.

The structures were solved by direct methods using the SHELXTL 6.14 package[85] and for all the atoms of all the structures, including hydrogen atoms from the ligand for **3**, were found by difference Fourier syntheses. All non-hydrogen atoms were anisotropically refined on F^2. Hydrogen atoms were refined isotropically. For **2**, hydrogen atoms were included in calculated positions. CCDC-631492 (**2**) and -631493 (**3**) contain the supplementary crystallographic data for this paper. These data can be obtained free of charge The Cambridge Crystallographic Data Centre via www.ccdc.cam.ac.uk/data_request/cif.

Spectroscopic measurements: Absorption spectra were recorded on Cary 50 Probe UV/visible spectrometer with Perkin–Elmer Luminescence Cells with a path length of 1 cm. Luminescence lifetime measurements were recorded on a Perkin-Elmer LS-50B spectrometer at 293 K (without external temperature regulation). The luminescence lifetime τ_L was measured by recording the decay at the maximum of the emission spectra. The signals were analysed as single-exponential decays. The instrument settings were: gate-time = 10 ms, integration time = 1 s, flash count = 5 and proper slit widths were used for no saturation of the signal by using a different delay time. Luminescence lifetimes are the average of three independent experiments. Solutions of [Tb(dpaa)], [Eu(dpaa)], [Tb(dpaa)$_2$] and [Eu(dpaa)$_2$] for luminescence lifetime determination were prepared in situ by mixing appropriate volumes of Ln^{III} in mQ water or in D_2O (concentration was determined by titration with EDTA in acetate buffer with xylenol orange indicator) and dpaa (in 0.1 M Tris buffer (pH 7.4) or in D_2O (pH $\approx$ 7)). Solutions of [Tb(dpaa)] (10^{-5} M) and [Eu(dpaa)] (10^{-4} M) with a 2% excess of dpaa were used. The luminescence lifetime of [Eu(dpaa)$_2$] was determined by using a 10% excess of dpaa ([Eu] $\approx 4 \times 10^{-4}$ M, [dpaa] $\approx 8.8 \times 10^{-4}$ M) and the luminescence lifetime of [Tb(dpaa)$_2$] was determined by using a 110% excess of dpaa ([Tb] $\approx 1.10^{-3}$ M, [dpaa] $\approx 4.3 \times 10^{-3}$ M). As a result of the different quenching efficiencies of the O−H and O−D oscillators, the measurement of the Ln^{III} luminescence lifetimes τ in solutions of H_2O and D_2O allows an accurate estimation of the number of coordinated water molecules present in solution q by using the equation of Beeby and co-workers ($q = A_{Ln}(1/\tau H_2O - 1/\tau D_2O - \alpha_{Ln})$ with $A_{Tb} = 5$ ms, $A_{Eu} = 1.2$ ms, $\alpha_{Tb} = 0.06$ ms^{-1} and $\alpha_{Eu} = 0.25$ ms^{-1}),[44] (a corrected version of the empirical equation of Horrocks and Sudnick[45] that accounts for closely diffusing OH oscillators). Luminescence excitation and emission spectra were recorded on the same instrument (delay = 0.05 ms, gate-time = 10 ms, cycle-time = 200 ms, flash count = 1×10^{-6} M) for solutions of [Tb(dpaa)], [Eu(dpaa)], [Tb(dpa)$_3$] and [Eu(dpa)$_3$] to obtain quantum yield measurements that were prepared in situ by mixing appropriate volumes of Ln^{III} in mQ water or in deuterated water (concentration was determined by titration with EDTA in acetate buffer with xylenol orange indicator) and dpaa (in 0.1 M tris buffer (pH 7.4) or in D_2O (pH 6.7–6.9 adjusted with NaOD)) or dpa (in 0.1 M tris buffer (pH 7.4)). The quantum yields Φ were calculated using the equation $\Phi_x/\Phi_r = A_r(\tilde{\nu}) \cdot n_x^2 \cdot D_x / A_s(\tilde{\nu}) \cdot n_r^2 \cdot D_r$, where x is the sample, r the reference, A the absorbance, $\tilde{\nu}$ the excitation wavenumber, n the refractive index and D the integrated emitted intensity. The tris(dipicolinate) complexes [Eu(dpa)$_3^{3-}$] ($\Phi = 13.5\%$, $7.5 \cdot 10^{-5}$ M in Tris buffer 0.1 M) and [Tb(dpa)$_3^{3-}$] ($\Phi = 26.5.5\%$, $6.5 \cdot 10^{-5}$ M in Tris buffer 0.1 M) were used as references for the determination of quantum yields of the Eu- and Tb-containing samples, respectively.[86] The consistency of the data was checked by measuring the quantum yield of the tris(dipicolinate) against rhodamine 101 ($\Phi_{abs} = 100\%$ in ethanol)[87]and cresyl violet ($\Phi_{abs} = 54\%$ in methanol).[87]

Solutions of [Tb(dpaa)] (4 mM) in the presence of BSA (12% w/v; $C_{Tb(dpaa)} = 3.92$ mM, $C_{BSA} = 1.8074$ mM, pH 7.0) for lifetime determination were prepared in situ by mixing appropriate volumes of solutions of [Tb(dpaa)] (in water or D_2O at pH $\approx$ 7, adjusted with NaOH or NaOD) with BSA. Luminescence emission spectra were recorded as mentioned before by direct excitation of the metal ($\lambda_{ex} = 368$ nm) and indirect excitation through the ligand ($\lambda_{ex} = 273$ nm).

Relaxivity measurements: The samples were prepared in situ by mixing the appropriate amounts of ligand and $GdCl_3 \cdot 6H_2O$ (99.99%; Aldrich) in water (mQ or D_2O) followed by adjustment of the pH value to approximately 7 with NaOH solution. The exact concentration of the Gd^{III} ions was determined by colourimetric titration in acetate buffer (pH 4.5) by using a standardised H_2Na_2(edta) solution (Aldrich) and xylenol orange as the indicator. The absence of free gadolinium was checked by the xylenol orange test.[88] The $1/T_1$ measurements were performed on a Brucker Avance 200 spectrometer (200 MHz).

Stock solutions ($\approx$ 2 M) of each anion (sodium hydrogen phosphate, potassium bicarbonate, sodium lactate, potassium oxalate, sodium acetate and citric acid) were prepared by dissolving a precisely preweighed mass of the respective acid or salt in D_2O and neutralising it to pD $\approx$ 7.4 with KOD or DCl solutions. The relaxivity that results from the [Gd(dpaa)(D$_2$O)$_3$] complex in the presence of anions was measured in solutions prepared by mixing appropriate volumes of the [Gd(dpaa)(D$_2$O)$_3$] and the anion stock solutions. The relaxivity at 200 MHz was compared to that of pure D_2O at the same pD value. For determination of the anion binding constant, the [Gd(dpaa)(D$_2$O)$_3$]/bicarbonate solution was titrated with incremental addition of the pure [Gd(dpaa)(D$_2$O)$_3$] complex at the identical pH value ($C_{Gd} = 0.51$ mM), and the relaxivity at 200 MHz was measured after each addition.

For the determination of the BSA binding constant, six solutions of [Gd(dpaa)$(H_2O)_3$] ($C_{Gd}=0.205$ mM, $C_{dpaa}=0.227$ mM) in pure H_2O at pH 7.0 (after adjustment with a NaOH solution) were prepared with various BSA concentrations (0–1.82 mM). The T_1 and T_2 measurements were performed at 60 MHz and 298 K in a Drusch electromagnet operated with the help of an Apollo tecmag console.

Theory

High-field relaxometry: This section presents a theoretical framework for evaluating the geometric and dynamic molecular factors that explain the water-proton high-field relaxivity with the minimal experimental work. It will be shown that such a characterisation can be done on a routine high-resolution spectrometer available to any chemistry laboratory interested in the synthesis of contrast agents. An important simplification that occurs in the interpretation of the measured relaxivities is that they are independent of the relaxation of the Gd^{III} electronic spin, the accurate description of which requires particular caution.[76] The longitudinal relaxation rate $R_1\equiv 1/T_1$, transverse relaxation rate $R_2\equiv 1/T_2$ and longitudinal relaxation rate in the rotating frame $R_{1,\sigma}\equiv 1/T_{1,\sigma}$ of a nuclear spin I can be measured in an external magnetic field B_0 by standard sequences.[89] The reference rates in the diamagnetic solution corresponding to the absence of Gd–L complexes are denoted by $R_{\alpha 0}\equiv 1/T_{\alpha 0}$ ($\alpha=1, 2, 1\rho$). Because of the large magnetic moment of the Gd^{III} centre, as a result of its electronic spin $S=7/2$, the observed relaxation rates R_α increase markedly with the concentration [GdL] (mM) of the Gd–L complexes added to the solution. The relaxivities r_α (s^{-1} mM^{-1}) are defined as the paramagnetic relaxation enhancements (PREs) $R_{\alpha p}\equiv R_\alpha - R_{\alpha 0}$ per mM of added Gd–L complex [Eq. (15)]:

$$r_\alpha \equiv R_{\alpha p}/[\mathrm{GdL}] \tag{15}$$

For the majority of polyaminocarboxylate complexes, the water molecules do not bind to the ligand and the high-field relaxivities of the water protons are conveniently ascribed to the populations of water molecules in the IS and OS hydration shells[7,66,77] of the Gd^{III} centre. More precisely, within the standard model of relaxivity, the IS contribution r_α^{IS} to the relaxivity r_α depends on 1) the number of water molecules q coordinated to the Gd^{III} centre, 2) the Gd–proton distance r_H of coordinated water, 3) the rotational correlation time $\tau_R\equiv 1/(6D_S{}^R)$ of the Gd–L complex of the rotational diffusion coefficient $D_S{}^R$ and 4) the coordination lifetime τ_M of a water molecule. The OS contribution r_α^{OS} depends on 5) the distance of closest approach a_{GdH} between the Gd^{III} nucleus and the protons of the OS water molecules and 6) the relative diffusion coefficient D of Gd–L and water. It will be shown that measuring the relaxivities r_1 and r_2, or equivalently $r_{1,\sigma}$, at a single high-field B_0 both for the water and CH_3 methanol protons is sufficient to evaluate the contributions of the IS and OS processes provided that the self-diffusion coefficients of water and methanol are known. Furthermore, assume that the IS Gd–proton distance has the probable value[55] $r_H=3.1$ Å. Then, once the number q of coordinated water molecules has been derived, for example from luminescence lifetime studies,[44,45] the remaining parameters τ_R, τ_M, a_{GdH} and D of the GdL/water and Gd—L/methanol pairs will be estimated from the measured r_1 and r_2 values of water and methanol. This analysis of the experimental data rests on the following high-field theory.

Let γ_I and γ_S be the gyromagnetic ratios of the spins I and S and $\omega_I\equiv 2\pi\vartheta_I\equiv|\gamma_I|B_0$ and $\omega_S\equiv 2\pi\vartheta_S\equiv|\gamma_S|B_0$ their angular Larmor frequencies. The dipolar coupling constant is defined in Equation (16):

$$A\equiv\frac{8\pi}{5}\gamma_I^2\gamma_S^2\hbar^2 S(S+1) \tag{16}$$

The relaxivity r_α ($\alpha=1, 2, 1\rho$) is the sum of the IS and OS contributions [Eq. (17)]:

$$r_\alpha = r_\alpha^{IS} + r_\alpha^{OS} \tag{17}$$

In the case of the water protons, the IS relaxivity is given[7,66,77] by Equations (18)–(20):

$$r_\alpha^{IS}=\frac{Pq}{T_{\alpha M}+\tau_M} \tag{18}$$

where $P\equiv 10^{-3}\,M/55.5\,M=1.8\times10^{-5}$ is the number of Gd–L complexes per water molecule and $T_{\alpha M}$ is the relaxation time of type α of the protons of a water molecule in the limiting situation in which it would be coordinated to the Gd^{III} centre for an infinite duration. In the case of the CH_3 protons of methanol, which does not coordinate to the Gd^{III} species, we have: $r_\alpha^{IS}=0$. The intramolecular relaxation rates $1/T_{\alpha M}$ are given by Equation (19a and b):

$$1/T_{1M}=Aj_{2c}^{IS}(i\omega_I) \tag{19a}$$

$$1/T_{2M}=1/T_{1\rho M}=A\left[\frac{2}{3}j_{2c}^{IS}(0)+\frac{1}{2}j_{2c}^{IS}(i\omega_I)\right] \tag{19b}$$

where the IS spectral density $j_{2c}^{IS}(\sigma)$ of complex (c) arguments $\sigma=i\omega$ ($\omega=0$ and ω_I) is defined by Equation (20):

$$j_{2c}^{IS}(\sigma=i\omega)=\frac{1}{4\pi r_H^6}\frac{\tau_R}{1+\omega^2\tau_R^2} \tag{20}$$

The following expressions of the OS relaxivities are valid for water and for any solute such as methanol that does not undergo long-range charge–charge interactions or binding with the Gd–L complex. The OS variation parameter λ_D is defined in Equation (21):

$$\lambda_D=\frac{8\pi}{45}\Gamma_I^2\gamma_S^2\hbar^2 S(S+1)10^{-6}N_{Avogadro} \tag{21}$$

At high field, the OS relaxivities take the simple forms[25,53] of Equation (22a and b):

$$r_1^{OS}=r_{mix}^{OS}(\infty)-(\lambda_D/D^{3/2})\sqrt{\pi\nu_I} \tag{22a}$$

$$r_2^{OS}=r_{1\rho}^{OS}=\frac{7}{6}r_{mix}^{OS}(\infty)-\frac{1}{2}(\lambda_D/D^{3/2})\sqrt{\pi\nu_I} \tag{22b}$$

where the mixed relaxivity $r_{mix}^{OS}(\infty)$ at infinite field $B_0=\infty$ is derived in Equation (23) to within a good approximation from the experimental high-field relaxivities as

$$r_{mix}^{OS}(\infty)=r_{mix}^{OS}=\frac{3}{2}\left(r_2^{OS}-\frac{1}{2}r_1^{OS}\right)=\frac{3}{2}\left(r_{1p}^{OS}-\frac{1}{2}r_1^{OS}\right) \tag{23}$$

In Equation (22), the universal dependence in $\sqrt{\nu_I}$ of the relaxivities stems from the fact that the long-time long-range relative translational diffusion of the water or solute molecule with respect to Gd–L has a 3D character and is independent of the details of the relative translational and rotational dynamics of the two interacting species when they are near one another. The determination of the infinite field value $r_{mix}^{OS}(\infty)$ of r_{mix}^{OS} from relaxivity measurements at a high, but finite field value B_0, is possible because r_{mix}^{OS} depends on the field, only through the longitudinal relaxation rate $R_{1e}=1/T_{1e}$ of the Gd^{III} electronic spin, which has negligible effects on the relaxivities at high field. Furthermore, according to Equation (5) given in reference[53] and Equations (A17) and (A18) of the related Supporting Information, the mixed relaxivity $r_{mix}^{OS}(\infty)$ has a simple theoretical expression given by Equation (24) in terms of the relative diffusion coefficient D and the collision diameter b:

$$r_{mix}^{OS}(\infty)=Aj_2(0)=\frac{\hat{k}_{solv}}{Db} \tag{24}$$

where $j_2(0)$ is the zero-frequency value of the OS dipolar spectral density $j_2(\sigma)$. The auxiliary coefficient $\hat{k}_{solv}$ has been introduced to emphasise the $1/(Db)$ dependence of $r_{mix}(\infty)$. The spectral density $j_2(0)$, and then $\hat{k}_{solv}$, depend on the pair-distribution function g_{IS} of M_I and Gd–L and on the eccentricity vectors ρ_I and ρ_S that give the positions of the spins I and S with respect to the molecule centres in the molecular frames of M_I and

Gd–L.[90–92] The radii of water, methanol and Gd–L are taken to be those of the spheres of the same volumes as the smallest ellipsoids containing these species. The methanol radius a_I(methanol)≅2 Å is not much larger than the water radius a_I(water)≅1.4 Å, and both molecules are significantly smaller than the complexes [Gd(dpaa)$(H_2O)_3$] and [Gd(dpaa)$_2$-(H_2O)]$^{3-}$ of radius a_S=4.1 and 5.1 Å, respectively. The collision diameter $b=a_I+a_S$ of a M_I/Gd–L pair is typically ≅6 Å. The eccentricity distances are ρ_I≅1 Å for water and methanol and ρ_S≅0 for Gd–L, so that the eccentricity parameters $(\rho_I/b)^2$ and $(\rho_S/b)^2$ have small values. The change of $\hat{k}_{solv}$ as a result of the spin eccentricities is typically given by a power series[91,92] of the eccentricity parameters and keeps modest both for water and methanol, so that the different eccentricity effects for these two molecules cannot cause an appreciable difference of their coefficients $\hat{k}_{solv}$. Furthermore, in the absence of charge–charge interactions,[93] the spectral density $j_2(0)$, and hence $\hat{k}_{solv}$, are weakly affected by the variation of the pair-distribution function g_{IS} induced by the changes in the sizes of M_I and Gd–L. Typically, assuming that water, methanol and Gd–L are hard spheres, the ratio of the $\hat{k}_{solv}$ coefficients for the methanol/Gd–L (m/GdL) and water/Gd–L (w/GdL) pairs is $\hat{k}_{solv}$(m/GdL)/$\hat{k}_{solv}$(w/GdL)=1 for centred spins with an accuracy better than 0.5%. The above discussion justifies the fundamental assumption $\hat{k}_{solv}$(m/GdL)=$\hat{k}_{solv}$(w/GdL). According to Equation (24), the products $r^{OS}_{mix}(\infty)Db$ have the same value for the methanol/GdL and water/GdL pairs as shown by Equation (25):

$$r^{OS}_{mix,m}(\infty)D_{m/GdL}b_{m/GdL} = r^{OS}_{mix,w}(\infty)D_{w/GdL}b_{w/GdL} \tag{25}$$

Adduct formation: Theoretical expressions of the longitudinal and transverse relaxivity changes as a result of the binding of the Gd–L complex to another species B will be derived in this section. The analytical concentrations (mol L^{-1}) of complex Gd–L and macromolecule B in the solution are denoted by c_{GdL} and c_B, respectively. The complex name may be abbreviated into C=Gd–L to simplify the notation. The two situations considered herein are the simple formation of a ternary adduct with a small species B, such as an oxyanion, according to Equation (26):

$$[BC] = K[B][C] \tag{26}$$

where K is the equilibrium constant and the more general binding of several complexes C to a macromolecule B, such as a protein with n equivalent binding sites 1, 2, …n. The sites are assumed to be well separated so that they bind the complexes C independently. Assume that $p-1$ complexes ($1\le p\le n$) are bound to B at the different sites i_1, i_2, …, i_{p-1} ($1\le i_1\le n$, …, $1\le i_{p-1}\le n$) to form the definite $(p-1)$-adduct B(i_1,…,i_{p-1})C$_{p-1}$. The binding of another complex C at a vacant site i_p of B to form the definite p-adduct B(i_1, …, i_p)C$_p$ satisfies the formation equilibrium defined by Equation (27):

$$[B(i_1,\cdots,i_p)C_p] = k[B(i_1,\cdots,i_{p-1})C_{p-1}][C] \tag{27}$$

where k is the binding equilibrium constant per site. Let BC$_p$ represent all the p-adducts made of the macromolecule B and of p complexes irrespective of the binding sites i_1, i_2, …, i_p. As all the sites are assumed to be equivalent, the concentration of BC$_p$ is given by Equation (28):

$$[BC_p] = \sum_{1\le i_1\le n,\cdots,1\le i_p\le n} [B(i_1,\cdots,i_p)C_p] = \binom{n}{p}[B(1,\cdots,p)C_p] \tag{28}$$

where $\binom{n}{p}$ is a binomial coefficient. The p-step formation constant K_p and the overall formation constants β_p are defined by Equation (29):

$$K_p \equiv \frac{n-p+1}{p}k \text{ and } \beta_p \equiv K_1K_2\cdots K_p \tag{29}$$

According to Equations (27) and (28), the concentration of BC$_p$ is given in terms of the concentrations [B] and [C] of free macromolecule B and complex C by Equation (30):

$$[BC_p] = \beta_p[B][C]^p \tag{30}$$

Substituting the expressions (30) for BC^p in the equations of conservation of the species B and C, the equilibrium concentration $[C]_{eq}$ of free complex is the solution of Equation (31):

$$f([C]) = [C] + \frac{\sum_{p=1}^{n} p\beta_p[C]^p}{1+\sum_{p=1}^{n}\beta_p[C]^p}c_B - c_{GdL} = 0 \tag{31}$$

Since $f(0)=-c_{GdL}<0$ and $f(c_{GdL})>0$, the numerical solution $[C]_{eq}$ of Equation (31) is readily obtained with the help of the bisection and/or false position methods.[94] Thus, in a solution of water containing C and B, the mean number $\bar{q}$ of metal-bound water molecules is given by Equation (32):

$$\bar{q} = \frac{[C]_{eq}}{c_{GdL}}q^{(f)} + \left(1-\frac{[C]_{eq}}{c_{GdL}}\right)q^{(b)} \tag{32}$$

where $q^{(f)}$ and $q^{(b)}$ are the numbers of metal-bound water molecules for the free (f) and bound (b) complex, respectively. Similarly, the mean relaxivity $\bar{r}_\alpha$ (α=1, 2, 1 ρ) of the water protons in that solution is given by Equation (33)

$$\bar{r}_\alpha = \frac{[C]_{eq}}{c_{GdL}}r_\alpha^{(f)} + \left(1-\frac{[C]_{eq}}{c_{GdL}}\right)r_\alpha^{(b)} \tag{33}$$

where $r_\alpha^{(f)}$ and $r_\alpha^{(b)}$ are the relaxivity values for the free and bound complex, respectively. The number $q^{(f)}$ of metal-bound water molecules and the relaxivity $r_\alpha^{(f)}$ for the free complex can be measured in the absence of species B.

Note that the formation of a ternary adduct of Gd–L with a small species B according to Equation (26) is a particular case of the general binding of several complexes C to a species B with n equivalent binding sites that correspond to $n=1$ and $K=k$.

Acknowledgements

This research was carried out in the frame of the EC COST Action D-38 "Metal-Based Systems for Molecular Imaging Applications" and the European Molecular Imaging Laboratories (EMIL) network. We thank Colette Lebrun for recording the mass spectra and Dr. Armel Guillermo for advice on using the Drusch electromagnet and the Apollo tecmag console.

[1] E. Toth, L. Helm, A. Merbach, *The Chemistry of Contrast Agents in Medical Magnetic Resonance Imaging, 1st ed.*, Wiley, Chichester, **2001**.
[2] M. P. Lowe, *Aust. J. Chem.* **2002**, *55*, 551–556.
[3] P. Caravan, *Chem. Soc. Rev.* **2006**, *35*, 512–523.
[4] S. Aime, S. G. Crich, E. Gianolio, G. B. Giovenzana, L. Tei, E. Terreno, *Coord. Chem. Rev.* **2006**, *250*, 1562–1579.
[5] D. A. Fulton, E. M. Elemento, S. Aime, L. Chaabane, M. Botta, D. Parker, *Chem. Commun.* **2006**, 1064–1066.
[6] M. Botta, *Eur. J. Inorg. Chem.* **2000**, 399–407.
[7] P. Caravan, J. J. Ellison, T. J. McMurry, R. B. Lauffer, *Chem. Rev.* **1999**, *99*, 2293–2352.
[8] S. Aime, A. Barge, M. Botta, J. A. K. Howard, R. Kataky, M. P. Lowe, J. Moloney, D. Parker, A. S. de Sousa, *Chem. Commun.* **1999**, 1047–1048.
[9] S. Aime, E. Gianolio, E. Terreno, G. B. Giovenzana, R. Pagliarin, M. Sisti, G. Palmisano, M. Botta, M. P. Lowe, D. Parker, *J. Biol. Inorg. Chem.* **2000**, *5*, 488–497.

[10] C. Geraldes, A. D. Sherry, P. Vallet, F. Maton, R. N. Muller, T. D. Mody, G. Hemmi, J. L. Sessler, *J. Mater. Chem. J. Magn. Res. Imag.* **1995**, *5*, 725–729.
[11] M. Botta, S. Aime, A. Barge, G. Bobba, R. S. Dickins, D. Parker, E. Terreno, *Chem. Eur. J.* **2003**, *9*, 2102–2109.
[12] E. Terreno, M. Botta, P. Boniforte, C. Bracco, L. Milone, B. Mondino, F. Uggeri, S. Aime, *Chem. Eur. J.* **2005**, *11*, 5531–5537.
[13] P. Caravan, J. C. Amedio, S. U. Dunham, M. T. Greenfield, N. J. Cloutier, S. A. McDermid, M. Spiller, S. G. Zech, R. J. Looby, A. M. Raitsimring, T. J. McMurry, R. B. Lauffer, *Chem. Eur. J.* **2005**, *11*, 5866–5874.
[14] R. S. Dickins, S. Aime, A. S. Batsanov, A. Beeby, M. Botta, J. Bruce, J. A. K. Howard, C. S. Love, D. Parker, R. D. Peacock, H. Puschmann, *J. Am. Chem. Soc.* **2002**, *124*, 12697–12705.
[15] L. Burai, V. Hietapelto, R. Kiraly, E. Toth, E. Brücher, *Magn. Reson. Med.* **1997**, *38*, 146–150.
[16] J. L. Sessler, T. D. Mody, G. W. Hemmi, V. Lynch, *Inorg. Chem.* **1993**, *32*, 3175–3187.
[17] D. Messeri, M. P. Lowe, D. Parker, M. Botta, *Chem. Commun.* **2001**, 2742–2743.
[18] S. Aime, L. Calabi, C. Cavallotti, E. Gianolio, G. Giovenzana, P. Losi, A. Maiocchi, G. Palmisano, M. Sisti, *Inorg. Chem.* **2004**, *43*, 7588–7590.
[19] S. Hajela, M. Botta, S. Giraudo, J. D. Xu, K. N. Raymond, S. Aime, *J. Am. Chem. Soc.* **2000**, *122*, 11228–11229.
[20] V. C. Pierre, M. Botta, S. Aime, K. N. Raymond, *Inorg. Chem.* **2006**, *45*, 8355–8364.
[21] C. J. Sunderland, M. Botta, S. Aime, K. N. Raymond, *Inorg. Chem.* **2001**, *40*, 6746–6756.
[22] A. Borel, H. Kang, C. Gateau, M. Mazzanti, R. B. Clarkson, R. L. Belford, *J. Phys. Chem. A* **2006**, *110*, 12434–12438.
[23] A. Nonat, C. Gateau, P. H. Fries, M. Mazzanti, *Chem. Eur. J.* **2006**, *12*, 7133–7150.
[24] E. Balogh, M. Mato-Iglesias, C. Platas-Iglesias, E. Toth, K. Djanashvili, J. A. Peters, A. de Blas, T. Rodriguez-Blas, *Inorg. Chem.* **2006**, *45*, 8719–8728.
[25] P. H. Fries, C. Gateau, M. Mazzanti, *J. Am. Chem. Soc.* **2005**, *127*, 15801–15814.
[26] N. Chatterton, C. Gateau, M. Mazzanti, J. Pécaut, A. Borel, L. Helm, A. E. Merbach, *Dalton Trans.* **2005**, 1129–1135.
[27] C. Platas-Iglesias, M. Mato-Iglesias, K. Djanashvili, R. N. Muller, L. V. Elst, J. A. Peters, A. de Blas, T. Rodriguez-Blas, *Chem. Eur. J.* **2004**, *10*, 3579–3590.
[28] C. Gateau, M. Mazzanti, J. Pécaut, F. Dunand, A. L. Helm, *Dalton Trans.* **2003**, 2428–2433.
[29] Y. Bretonnière, M. Mazzanti, F. A. Dunand, A. E. Merbach, J. Pécaut, *Chem. Commun.* **2001**, 621.
[30] Y. Bretonnière, M. Mazzanti, F. A. Dunand, A. E. Merbach, J. Pécaut, *Inorg. Chem.* **2001**, *40*, 6737–6745.
[31] R. Wietzke, M. Mazzanti, J.-M. Latour, J. Pécaut, P.-Y. Cordier, C. Madic, *Inorg. Chem.* **1998**, *37*, 6690–6697.
[32] C. F. G. C. Geraldes, M. C. Alpoim, M. P. M. Marques, A. D. Sherry, M. Singh, *Inorg. Chem.* **1985**, *24*, 3876–3881.
[33] Z. Zheng, *Chem. Commun.* **2001**, 2521–2529.
[34] L. Natrajan, J. Pécaut, M. Mazzanti, *Dalton Trans.* **2006**, 1002–1005.
[35] L. Natrajan, J. Pécaut, M. Mazzanti, C. LeBrun, *Inorg. Chem.* **2005**, *44*, 4756–4765.
[36] A. S. W. Bligh, N. Choi, E. Evagourou, G. , M. McPartlin, K. N. White, *J. Chem. Soc. Dalton Trans.* **2001**, 3169–3172.
[37] W. K. Wong, L. L. Zhang, F. Xue, T. C. W. Mak, *J. Chem. Soc. Dalton Trans.* **1999**, 3053–3062.
[38] W. J. Evans, G. W. Rabe, J. W. Ziller, *Inorg. Chem.* **1994**, *33*, 3072–3078.
[39] A. J. Stemmler, J. W. Kampf, M. L. Kirk, B. H. Atasi, V. L. Pecoraro, *Inorg. Chem.* **1999**, *38*, 2807–2817.
[40] A. Bianchi, L. Calabi, F. Corana, S. Fontana, P. Losi, A. Maiocchi, L. Paleari, B. Valtancoli, *Coord. Chem. Rev.* **2000**, *204*, 309–393.
[41] G. Anderegg, F. Wenk, *Helv. Chim. Acta* **1967**, *50*, 2330–2332.
[42] G. R. Choppin, P. Thakur, J. N. Mathur, *Coord. Chem. Rev.* **2006**, *250*, 936–947.
[43] L. C. Thompson, J. A. Loraas, *Inorg. Chem.* **1963**, *2*, 89–93.
[44] A. Beeby, I. M. Clarkson, R. S. Dickins, S. Faulkner, D. Parker, L. Royle, A. S. de Sousa, G. J. A. Williams, M. Woods, *J. Chem. Soc. Perkin Trans. 2* **1999**, 493–503.
[45] W. D. Horrocks, Jr., D. R. Sudnick, *Acc. Chem. Res.* **1981**, *14*, 384–392.
[46] W. D. Horrocks, Jr., D. R. Sudnick, *J. Am. Chem. Soc.* **1979**, *101*, 334–340.
[47] V. S. Sastri, J.-C. Bünzli, V. Ramachandra Rao, G. V. S. Rayudu, J. R. Perumareddi, *Modern Aspects of Rare Earths and Their Complexes*, Elsevier, Amsterdam, **2003**.
[48] F. Benetollo, G. Bombieri, L. Calabi, S. Aime, M. Botta, *Inorg. Chem.* **2003**, *42*, 148–157.
[49] L. I. Semenova, A. N. Sobolev, W. B. Skelton, A. H. White, *Aust. J. Chem.* **1999**, *52*, 507–517.
[50] G. Geier, U. Karlen, *Helv. Chim. Acta* **1971**, *54*, 135–143.
[51] R. B. Lauffer, *Chem. Rev.* **1987**, *87*, 901–927.
[52] A. Jerschov, N. Muller, *J. Magn. Reson.* **1997**, *125*, 372–375.
[53] A. Melchior, P. H. Fries, *J. Am. Chem. Soc.* **2006**, *128*, 7424–7425.
[54] L. Vander Elst, A. Sessoye, S. Laurent, N. R. Muller, *Helv. Chim. Acta* **2005**, *88*, 574–587.
[55] P. Caravan, A. V. Astashkin, A. M. Raitsimring, *Inorg. Chem.* **2003**, *42*, 3972–3974.
[56] A. Nonat, L. Helm, M. Mazzanti, unpublished results; H. D. Powell, O. M. N. Ni Dhubhghaill, D. Pubanz, L. Helm, Y. S. Lebedev, W. Schlaepfer, A. E. Merbach, *J. Am. Chem. Soc.* **1996**, *118*, 9333–9346.
[57] F. A. Dunand, A. Borel, L. Helm, *Inorg. Chem. Commun.* **2002**, *5*, 811–815.
[58] A. C. Chang, H. G. Brittain, J. Telser, M. F. Tweedle, *Inorg. Chem.* **1990**, *29*, 4468–4473.
[59] S. Rast, A. Borel, L. Helm, E. Belorizky, P. H. Fries, A. E. Merbach, *J. Am. Chem. Soc.* **2001**, *123*, 2637–2644.
[60] Y. Ayant, E. Belorizky, E. Alison, J. Gallice, *J. Phys. Chem. Solids J. Phys. (France)* **1975**, *36*, 991–1004.
[61] L. Hwang, J. H. Freed, *J. Chem. Phys.* **1975**, *63*, 4017–4025.
[62] W. P. Cacheris, S. C. Quay, S. M. Rockalage, *Magn. Reson. Imaging* **1990**, *8*, 467–481.
[63] S. Aime, M. Botta, I. J. Bruce, V. Mainero, D. Parker, E. Terreno, *Chem. Commun.* **2001**, 115–116.
[64] J. I. Bruce, R. S. Dickins, L. J. Govenlock, T. Gunnlaugsson, S. Lopinski, M. P. Lowe, D. Parker, R. D. Peacock, J. J. B. Perry, S. Aime, M. Botta, *J. Am. Chem. Soc.* **2000**, *122*, 9674–9684.
[65] H. A. Krebs, *Annu. Rev. Biochem.* **1950**, *19*, 409–430.
[66] A. E. Merbach, E. Toth, *The Chemistry of Contrast Agents in Medical Magnetic Resonance Imaging*, Wiley, Chichester, **2001**.
[67] D. M. J. Doble, M. Melchior, B. O'Sullivan, C. Siering, J. D. Xu, V. C. Pierre, K. N. Raymond, *Inorg. Chem.* **2003**, *42*, 4930–4937.
[68] R. B. Lauffer, *Magn. Reson. Med.* **1991**, *22*, 339–342.
[69] S. Aime, M. Botta, M. Fasano, G. S. Crich, E. Terreno, *J. Biol. Inorg. Chem.* **1996**, *1*, 312–319.
[70] P. Caravan, N. J. Cloutier, M. T. Greenfield, S. A. McDermid, S. U. Dunham, J. W. M. Bulte, J. C. Amedio, R. J. Looby, R. M. Supkowski, W. D. Horrocks, T. J. McMurry, R. B. Lauffer, *J. Am. Chem. Soc.* **2002**, *124*, 3152–3162.
[71] P. Caravan, C. Comuzzi, W. Crooks, T. J. McMurry, G. R. Choppin, S. R. Woulfe, *Inorg. Chem.* **2001**, *40*, 2170–2176.
[72] M. H. Ou, C. H. Tu, S. C. Tsai, W. T. Lee, G. C. Liu, Y. M. Wang, *Inorg. Chem.* **2006**, *45*, 244–254.
[73] M. K. Thompson, D. M. J. Doble, L. S. Tso, S. Barra, M. Botta, S. Aime, K. N. Raymond, *Inorg. Chem.* **2004**, *43*, 8577–8586.
[74] J. Hamblin, N. Abboyi, M. P. Lowe, *Chem. Commun.* **2005**, 657–659.
[75] I. Bertini, C. Luchinat, G. Parigi, *Solution NMR of Paramagnetic Molecules*, Elsevier, Amsterdam, **2001**.
[76] P. H. Fries, E. Belorizky, *J. Chem. Phys.* **2005**, *123*, 124510–124515.
[77] S. Aime, M. Botta, E. Terreno, *Adv. Inorg. Chem.* **2005**, *57*, 173–237.
[78] A. Borel, L. Helm, A. E. Merbach, *Chem. Eur. J.* **2001**, *7*, 600–610.

[79] R. Fornasier, D. Milani, P. Scrimin, U. Tonellato, *J. Chem. Soc. Perkin Trans. 2* **1986**, 233–237.
[80] K. Mikkelsen, S. O. Nielsen, *J. Phys. Chem.***1960**, *64*, 632–637.
[81] A. E. Martell, R. M. Smith, *Critical Stability Constants, Vol. 4*, Plenum Press, New York, **1976**.
[82] P. Gans, A. Sabatini, A. Vacca, *Talanta* **1996**, *43*, 1739–1753.
[83] P. Gans, A. Sabatini, A. Vacca, University of Leeds and University of Florence, Leeds, UK and Florence, Italy, **2000**.
[84] Bruker, Madison, WI, USA, **1995**.
[85] G. M. Sheldrick, 6.14 ed., University of Göttingen, Germany, Germany, **2006**.
[86] A.-S. Chauvin, F. Gumy, D. Imbert, J.-C. Bünzli, *Spectrosc. Lett.* **2004**, *37*, 517–532.
[87] D. F. Eaton, *Pure Appl. Chem.* **1988**, *60*, 1107.
[88] G. Brunisholz, M. Randin, *Helv. Chim. Acta* **1959**, *42*, 1927–1938.
[89] D. Canet, *Adv. Inorg. Chem.* **2005**, *57*, 3–40.
[90] Y. Ayant, E. Belorizky, P. Fries, J. Rosset, *J. Phys. (France)* **1977**, *38*, 325–337.
[91] P. Fries, E. Belorizky, *J. Phys. (France)* **1978**, *39*, 1263–1282.
[92] P. H. Fries, B. Melloni-Rigobello, *J. Phys. (France)* **1982**, *43*, 1397–1405.
[93] P. H. Fries, G. N. Patey, *J. Chem. Phys.* **1984**, *80*, 6253–6266.
[94] W. H. Press, B. P. Flannery, S. A. Teukolsky, W. T. Vetterling, *Numerical Recipes. The Art of Scientific Computing*, Cambridge University Press, Cambridge, **1990**.

Received: December 21, 2006
Revised: March 22, 2007
Published online: July 20, 2007

